Università degli Studi di Milano - Bicocca
Scuola di Scienze
Dipartimento di Scienza dei Materiali
Corso di Laurea Magistrale in Materials Science

Study of diffusion coefficient and decay time of a molecular rotor in polymeric matrices

Relatore: Prof. Roberto Simonutti
Correlatore: Dr. Michele Mauri

Relazione della prova finale di:

Valeria Vanoli

Matricola 767230

Anno Accademico 2018/2019

Contents

Chapter 1

Introduction

The present thesis work is based on the study of the behavior of a molecular rotor, LBX37, dispersed in different polymeric matrices, though fluorescence correlation spectroscopy (FCS) and Time-Correlation Photon Counting (TCSPC) measurements, performed at the Max Planck Institute fur Polymerforschung in Mainz, Germany.

Molecular rotors are a group of fluorescent molecules that form twisted intramolecular charge transfer (TICT) states upon photoexcitation. When intramolecular twisting occurs, the molecular rotor returns to the ground state either by emission of a red-shifted emission band or by nonradiative relaxation. The emission properties are strongly solvent-dependent, and the solvent viscosity is the primary determinant of the fluorescent quantum yield from the planar (non-twisted) conformation. This viscosity-sensitive behavior gives rise to applications in, for example, fluid mechanics, polymer chemistry, cell physiology, and the food sciences.

Monitoring the behavior of small fluorescent tracers dispersed in a polymer matrix is a powerful approach to obtain important insights on the polymer sys-

tem properties. A number of fluorescent based techniques including fluorescence correlation spectroscopy, fluorescence recovery after photobleaching or fluorescent lifetime measurements can be used for such studies. In particular, fluorescence correlation spectroscopy (FCS) can be used to measure the translational diffusion coefficient of the tracers and correlate it to the segmental mobility of bulk homopolymers, to the local composition of polymer blends or to crowding effects in polymers solutions and gels.
Fluorescence lifetime measurements can be made using time correlated single photon counting technique, which is a technique that measures the arrival of a single photon that allows to obtain the lifetime and the decay shape of a molecule.

The aim of this project is to directly compare the information that can be obtained by FCS and TCSPC using identical polymer matrices and fluorescent tracers. In the specific, the NAME? molecular rotor was used in the study. We studied different polymers with glass transition temperatures going from -100°C to about -10°C. Moreover, each polymer was analyzed over a range of molecular weights.
Each sample was prepared mixing 100μL of rotor dissolved in pure chloroform at a concentration of 10-8M in 100mg of pure polymer. The solution was stirred for 24h and then placed in an oven at 50°C under vacuum for another 24h. As a sample holder an Attofluor® cell chamber (Invitrogen, Paisley, UK) was used.

Time-correlated single photon counting (TCSPC) data were recorded on a confocal setup. A PicoQuant diode laser (λ=405 nm) was coupled into a Zeiss LSM 880 microscope (Carl Zeiss, Jena, Germany) using a MBS405 dichroic mirror (Carl Zeiss, Jena, Germany). Analysis of the TCSPC data was performed using the PicoQuant SymPhoTime 64 software.

FCS experiments were performed on an LSM 880 (Carl Zeiss, Jena, Germany) setup. A HeNe laser ($\lambda = 633$ nm) was used for excitation of all the samples and emission in the range from 500 to 553nm was detected.

Chapter 2

Physico-chemical Concepts and Methods

2.1 Fluorescence

Fluorescence is a widely used phenomenon, both in nature and in research. It is considered important for being the basic concept of various analytical methods, such as fluorescence spectroscopy and microscopy, which can be used in a wide variety of fields. In particular, the study of some molecules' fluorescence has become more and more important in various research fields, such as chemistry, physics, biotechnology or medical diagnostics. [2]

Fluorescence is a luminescence process, which consists in the emission of a photon from electronically excited states. Electrons in a molecule can be excited through the absorption of a photon with specific values of energy, which means that absorption (and emission) are only possible considering discrete increments of energy. To describe these processes, we use Jablonski diagrams (figure 2.1), which show singlet electronic states (S_0, S_1, S_2) and their numerous vibrational levels (0,

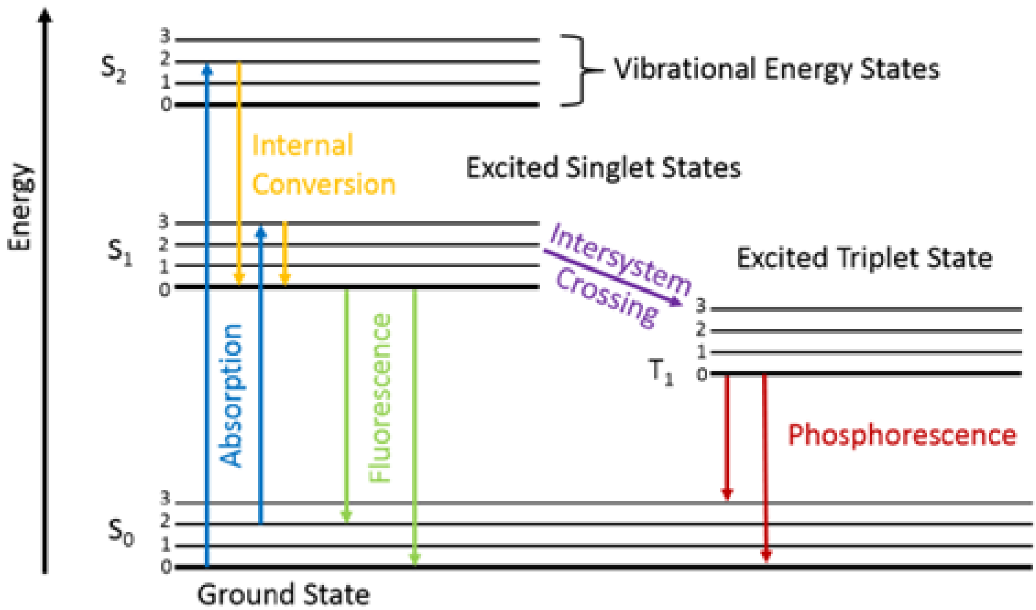

Figure 2.1: Jablonski diagram showing absorption and emission processes of both fluorescence and phosphorescence. Fluorescence happens when absorption and emission both occur between vibrational states of the singlet ground state S_0 and a singlet excited state (S_1, S_2..). Phosphorescence happens after the system undergoes an intersystem crossing process and, while absorption still happens between singlet states, the emission happens from a triplet state to the singlet ground state.

1, 2,...) as well as triplet states (T_1).

When a molecule absorbs a photon, it goes from its ground state S_0 to a higher energy level such as S_1 or S_2. After the absorption, the system can either undergo an internal conversion process or an intersystem crossing process. An intersystem crossing happens when an electron in the S_1 state undergoes a spin conversion process. From quantum theory, it is forbidden for an electron to be in any spin state other than the two existing in the paired electrons ($+\frac{1}{2}$ or $-\frac{1}{2}$); thus, for the electron to reverse its spin, it must go through a 'forbidden' transition, which is relatively unlikely. Nonetheless, electrons can undergo an 'intersystem crossing' between singlet and triplet states. [1]

Usually, the emission from this triplet state is shifted to longer wavelengths and is described as phosphorescence, with an average lifetime of $> 10^{-6}$ seconds. [3]

On the other hand, an internal conversion happens when the molecule relaxes from a higher energy level to the lowest vibrational level of S_1. The emission from the lowest vibrational level of energy of S_1 to the S_0 state is described as fluorescence. In the case of fluorescence, the electron in the excited orbital of the excited singlet state is paired to the electron in the ground state orbital. Hence, the return of the excited electron to the ground state is very fast and leads to the emission of a photon. The general fluorescence emission rates are around 10^8 s^{-1}. Typically, the absorption energy is higher than the emission energy, and fluorescence appears at respectively lower energies and longer wavelengths.[2]

The fluorescence lifetime τ of a compound is the average time the molecule stays in the excited state before returning to the ground state. Typically, fluorescence lifetimes are around 10 ns.[2]

It is important to keep in mind that the fluorescence of a molecule can be influenced by many environmental factors, such as surrounding solvent molecules, temperature, pH and localized concentration of the fluorescent species [2?], even though not all fluorophores are influenced in the same way.[2,3,4]

Some compounds that have a particularly strong absorption and emission (QY ?) are studied because of their fluorescent properties and are commonly called fluorophores.

The fluorescent dyes most commonly used for fluorescence spectroscopy applications are Alexa Fluor and Atto dyes. These molecules are made mainly of conjugated double bonds systems, often in the form of aromatic rings. [reference] Different absorption and emission spectra can be obtained just slightly changing the features of the molecules. For example, in case of Alexa Fluor dyes, a variety of different structure exist, which can be excited at wavelengths from 350 nm up to 790 nm.[5]

Another type of fluorophores that has gained importance over the last years are fluorescence molecular rotors, which will be described in detail in the next chapter.

2.2 Molecular rotor

As previously mentioned, commercially available fluorescent dyes are very useful for various applications and studies in the fields of microscopy and spectroscopy. A particular type of fluorescent dyes are the so called fluorescent molecular rotors (FMR). These molecules are fluorophores that can undergo an intramolecular twisting motion in the fluorescent excited state, activating a twisted intramolecular charge transfer process (TICT). [6,7]

The general structure of molecular rotors can be described as formed by three basic components: an electron donor unit, an electron acceptor unit and a π-conjugated electron-rich spacer [6,7] which allows the electron transfer between the two units in the planar configuration [8]. When a molecule with this structure is photo-excited (S_0-S_1), there is a TICT process from the donor to the acceptor unit and electrostatic forces induce an intramolecular twisting motion of both parts of the molecule around the σ-bond.

Relaxation from the TICT state can happen in two ways, as shown in figure 2.2.

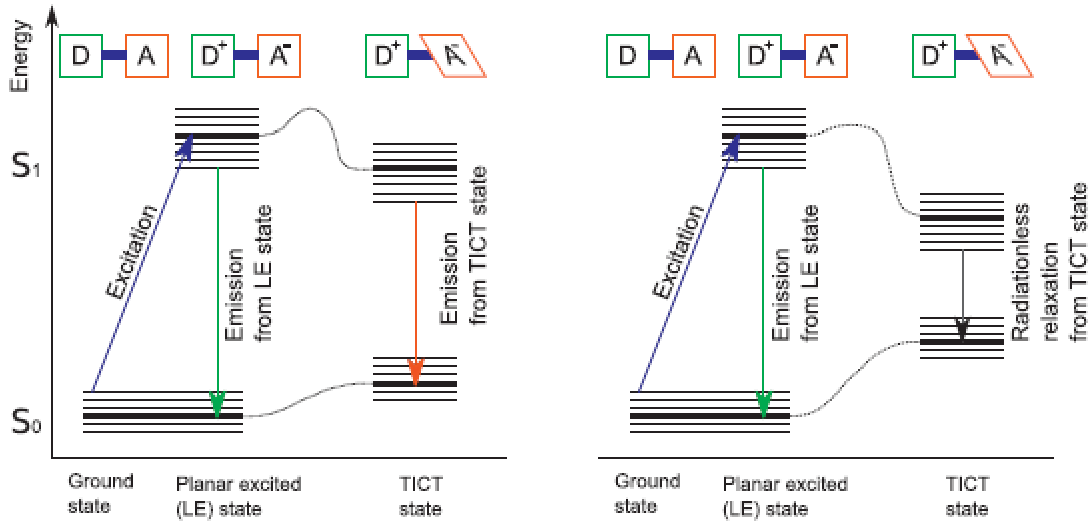

Figure 2.2: Scheme of the electronic states and possible relaxation process for a fluorescent molecular rotor. If the electron donor part (D) of the molecular rotor and the acceptor (A) are in the planar state, the excitation and emission process is the same as for conventional fluorophores. This is the case for a high viscosity environment, resulting in longer fluorescence lifetimes. For the twisted state of molecular rotors (in low viscosity environment), the Jablonski diagram needs to be extended. The excited-state energy for a twisting molecule is lower in the TICT state, whereas the ground-state energy is higher. The energy gab between these states is lower and the fluorescence lifetime is shorter.

In the first case, the S_1-S_0 energy gap in the twisted state is large enough to allow photon emission when the molecule goes back to the ground state, while still keeping the twisted conformation. In this case the fluorophore shows both the LE fluorescence emission band and a red-shifted second emission band and both processes lead to photon emission. On the other hand, when the TICT energy gap is much smaller than the LE energy gap, a non-radiative relaxation takes place from the TICT state and the fluorophore shows a single emission band. [6]

The spectroscopic properties of the molecular rotor are influenced by many aspects.

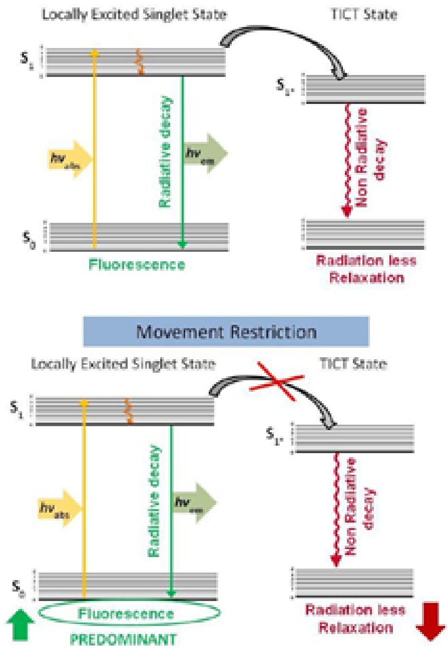

Figure 2.3: Jablonski diagram of a single emission band molecular rotor. Top: Notice that relaxation from the TICT state occurs without fluorescence emission. Bottom: Restriction of formation of the twisted state increases fluorescence emission.

First of all, the TICT of the rotor molecule has a strong dependence on the environment, and in particular on its viscosity. [6-10] The higher the viscosity of the environment and the more the twisted-state formation is hindered, which means that the non-radiative pathway is blocked and the fluorescent quantum-yield increases. [6,8]

Besides the viscosity and the polarity of the solvent, the formation of hydrogen bonds and the excimer formation should also be taken into account. Polar solvents, for example, stabilize the TICT state of the molecule and increase the relaxation time from this state. The polarity is linked to the ability to build hydrogen bonds, and the formation of these bonds between the molecule and the solvent increases the TICT formation rate. Nevertheless, the viscosity of the microenvironment of the molecule is often the dominating factor. [6,10]

There are different classes of FRM, such as push-pull type, BODIPY- based, cyanine-based, stilbenes or benzonitrile-based molecules. [7]

The molecule that was used in this project is called LBX37 (pictured in figure 2.4) is made of a naphthalene unit, the electron-acceptor and a dibenzoazepine unit, the electron-donor. [9]

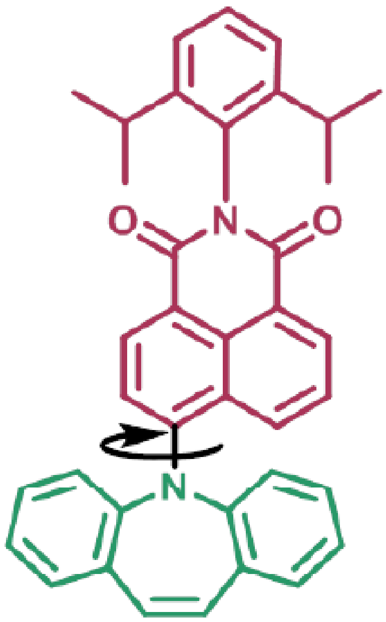

Figure 2.4: Chemical structure of the molecular rotor LBX37 used in this work. The molecule rotates around the axis of the C-N-bond between the naphthalene unit, which is the electron-acceptor (red upper part) and the dibenzoazepine unit, which is the electron-donor (green lower part).

FMR can be used as viscosity sensors in different fields, such as fluid mechanics, polymer chemistry and cell physiology. In biological research fields, molecular rotors have the advantage to result in a quantitative fluorescence response, compared to qualitative data for other fluorescent probes. [6]

In questo lavoro li abbiamo usati per studiarne i tempi di vita e I coefficient di diffusione in polimeri con diverse masse molecolari.

2.3 Time correlated single photon counting

Time-resolved fluorescence spectroscopy is one of the various fluorescence spectroscopy techniques that are interesting for both physics and life sciences. [8, 16, 17]

In this context is possible to introduce time-correlated single photon counting (TCSPC), which is a technique that measures the arrival of a single photon that allows to obtain the lifetime and the decay shape of a molecule. This method is also particularly interesting as it allows to work with both mono and multi-exponential decays.

The working mechanism is the following. A repeated impulse coming from a short-pulsed laser is used to excite the molecule, which then relaxes emitting a photon. The time between the excitation pulse and the arrival of the first emitted photon to the detector is measured, as shown in figure 2.5.A. This excitation-emission cycle is repeated many times, all the measurements are then registered and a histogram showing number of photons vs arrival time is produced (figure 2.5.C).

The use of several repetitions in this method prevents some problems that can be encountered using a single excitation-emission cycle. First of all, the decay time can be very fast, which makes it not so easy to detect. Moreover, the intensity may be too weak to be registered using transient electronic recorders [16].

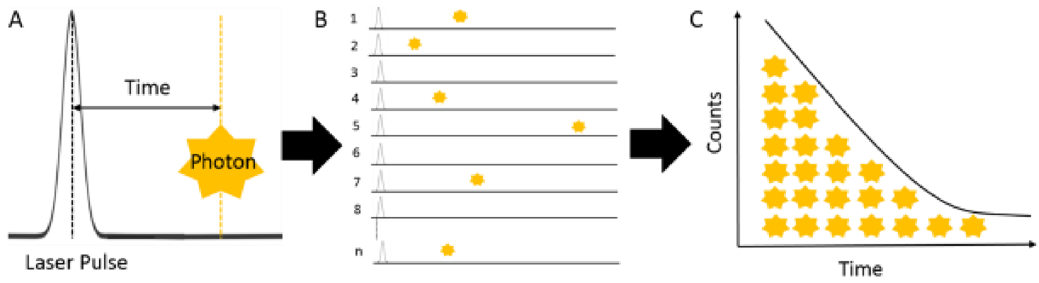

Figure 2.5: Principle of time-correlated single photon counting (TCSPC). (A) A fluorescent sample is excited repetitively by short laser pulses and the time between excitation and emission is measured. The laser pulse is the start and the first photon arrival at the detector is the stop. The time in between is measured. (B) This process is repeated many times to count the number of photons arriving at a certain time or time rage. (C) According to their arrival time, the photons are sorted into a histogram. Adapted from [15,16,29].

The histogram shows the intensity I plotted against the photon arrival time t. From this the fluorescence lifetime τ can be determined from the slope of the exponential decay fit function (equation 2.1).[8]

$$I_t = I_0 \times e^{(-\frac{t}{\tau})} \tag{2.1}$$

There are some cases in which the sample displays two different fluorescence lifetimes ($\tau 1$, $\tau 2$) and a mono-exponential fitting is not enough. In this case the decay curve is the sum of two intensity decay curves and can be expressed in a way that includes both fluorescence lifetimes:

$$I_t = I_{1,t=0} e^{(-\frac{t}{\tau_1})} + I_{2,t=0} e^{(-\frac{t}{\tau_2})} \tag{2.2}$$

The general term (equation 2.3) for samples with more than one lifetime is described with the amplitude A as:

$$I_t = \sum_{i=1}^{n} A_i e^{(-\frac{t}{\tau_i})} \tag{2.3}$$

For such samples, a weighted average fluorescence lifetime τ_{wa} can be defined. This lifetime takes the different single lifetimes τ_i as well as their amplitudes A_i into account as described by equation 2.4.

$$\tau_{wa} = \frac{\sum_{i=1}^{n} A_i \times \tau_i}{\sum_{i=1}^{n} A_i} \tag{2.4}$$

The resolution of TCSPC experiments is given by its instrument response function (IRF), that contains the pulse shape of the laser, the temporal dispersion in the optical system, the detector as well as the electronic characteristics.[16] Ideally, the IRF is infinitely narrow, due to an infinitely sharp excitation pulse and infinitely accurate detectors and electronics.

In this work, TCSPC was used to determine the fluorescence lifetime of the fluorescent molecular rotor LBX37, in order to monitor the formation process of nanoparticles via a solvent evaporation process.

2.4 Confocal laser scanning microscopy

Confocal laser scanning microscopy (CLSM) is a versatile tool to image fluorescently labeled probes [19] and was invented by M. Minsky in the 1950s. [20] It has proven to be of high value in different fields of study so that it has been continuously improved during the years. The universal application of CLSM is caused by the many advantages of the method: high resolution images, relatively high frame rates and 3D imaging in particular, are among the main features of CLSM. [18,19,20]

Confocal laser scanning microscopy can visualize fluorescently labeled probes in a 3D image showing details that were previously only seen in very thin samples using the conventional epifluorescence microscopes, as in thick samples the fluorescence background overwhelmed the focal plane signal. [19] Moreover, in contrast to standard epifluorescence microscopy, CLSM detects only fluorescence coming from the focal plane thanks to the presence of a pinhole which excludes out-of-focal-plane florescent signal. [18]

The principle, depicted in figure 2.6, is based on scanning the sample point by point using a laser beam that is focused into the sample. The laser light is scanned across the sample and the fluorescence signal is collected using the single objective lens. The optical path is designed so that when the laser beam is focused in the specimen, it is confocal with the point of light focused at the pinhole in front of the photodetector. Thus, only information from the focal plane of interest reaches the photodetector.[19]

The signal coming from the focal plane within the sample is detected by a photodetector, like a photomultiplier tube (PMT) or Avalanche photodiode (APD), behind the pinhole. A stepper motor or piezo-drive is used to go small steps along the z-axis to obtain three-dimensional information and images. [18]

There are different types of CLSM, which can be classified by the scanning process. 3D images can either be taken by stage-scanning or beam-scanning. The latter process is more suitable for biological probes, because image acquisition times are faster. [19]

Confocal laser scanning microscopy is used in many disciplines, such as biology,

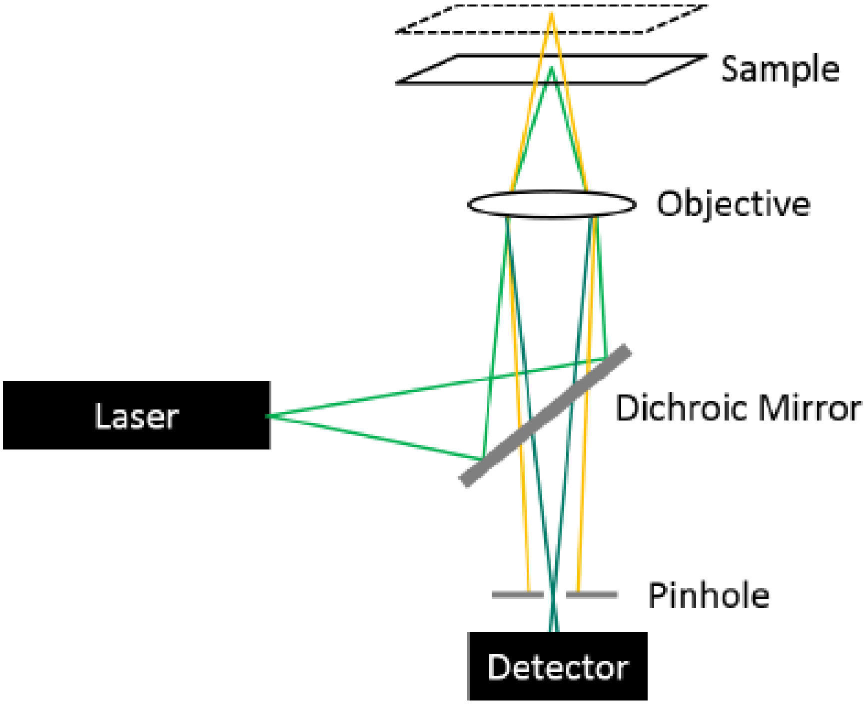

Figure 2.6: Optical path of a confocal laser scanning microscopy. The light coming from the laser is directed on the sample by a dichroic mirror. The emitted fluorescent signal is then collected by the detector using single objective lenses and passing through a pinhole that allows to remove unwanted fluorescence coming from the background. [8, 18]

medicine, chemistry, physics and material sciences.[8] The CLSM method itself is already a frequently used analysis tool, but CLSM is also the basic concept for many other methods, such as fluorescence correlation spectroscopy (FCS, described in the next section) or fluorescence lifetime imaging microscopy (FLIM).

2.5 Fluoresce correlation spectroscopy

Fluorescence correlation spectroscopy (FCS) is a technique developed in the early 1970s by Madge, Elson and Webb and became more and more interesting to researchers in the following years because of its wide range of possible applications, going from physical chemistry to biophysics. [8, 12-15] FCS investigates the dynamics of fluorescent molecules, nanoparticles or macromolecules and moreover it is compatible with a wide range of different solvents [13] which allows to study the behavior of fluorescent molecules in various environments.

The fundamental idea of FCS is taking advantage of the small spontaneous fluctuations of physical parameters that are somehow reflected by the fluorescence emission of the molecules diffusing in and out a very small observation volume, typically of about $1\mu m^3$. [13, 14]

From these fluctuations we can get an auto-correlation curve, which can be obtained by quantify the fluctuations' intensity by temporally auto-correlating the signal in order, as shown in figure 2.7.

From this correlation process, FCS allows to study the dynamics of the systems, analyzing parameters such as diffusion coefficients, diffusion time, hydrodynamic radii, concentration of particles or chemical reactions. [8,14] Another important feature is the technique's sensitivity, which allows to analyze individual the behavior of individual molecules.

2.5.1 Theory

As previously said, FCS relies on the analysis of spontaneous fluctuations in a laser-induced fluorescent signal. This analysis allows to obtain many information

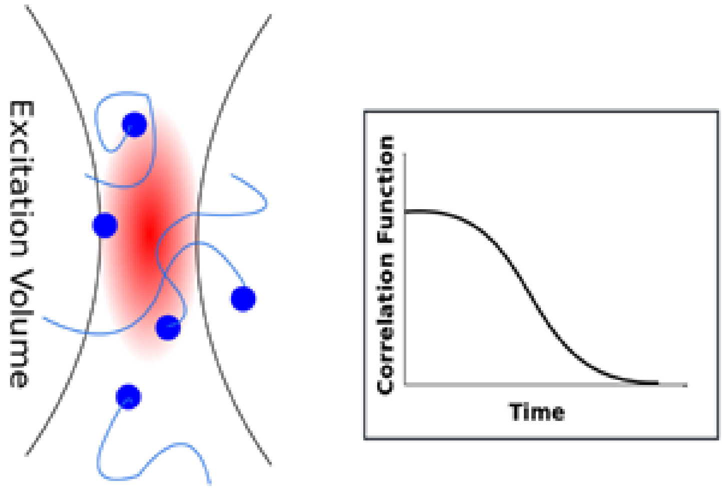

Figure 2.7: Graphic representation of how small fluorescence fluctuations happen (fluorescent molecules moving in and out of the excitation volume) and the resulting correlation curve that is obtained from the detected signal.

on the system, both microscopic and macroscopic.

We can define the fluctuations of a fluorescent signal as the deviation from the temporal average of the signal [12, 13, 15], as expressed by equation 2.5:

$$\delta F(t) = F(t) - <F(t)> \tag{2.5}$$

where the temporal average is given by

$$<F(t)> = \frac{1}{T}\int_0^T F(t)dt \tag{2.6}$$

The relaxation of these fluctuations around an equilibrium state can be described using a normalized second order auto-correlation function

$$G(\tau) = \frac{<\delta F(t)\delta F(t+\tau)>}{<\delta F(t)>^2} \tag{2.7}$$

This function compares the fluctuating signal at a time t with itself at a time t+τ, averaged over all times, which defines the self-similarity of the system. τ is called lag time. The process is depicted in figure 2.8.

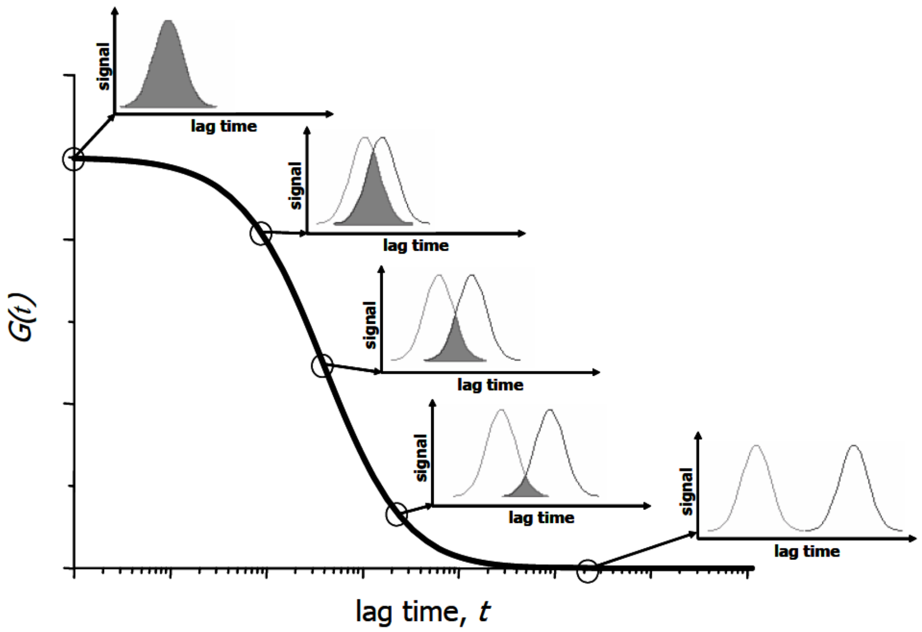

Figure 2.8: Graphic depiction of how lag time and a correlation curve are related. A short lag time corresponds to a high autocorrelatio which corresponds to high value of G(τ). Increasing the lag time, the level ofsutocorrelation decreases and so does the G(τ) value.

Let consider a case in which the fluctuations of the fluorescence signal are caused by the diffusion of a fluorophore in a defined observation volume. The level of self-similarity is related to the diffusion time of the fluorophore, and the decay of the corresponding autocorrelation curve represents the mobility of the fluorophore.

Measuring a short lag time means that the fluorophore will only move for small distances and so it will have a higher probability to stay inside the observation volume, which results in a high autocorrelation; on the contrary, a long lag time means that the fluorophore has likely diffused out of the observation volume so the self-similarity is low and the autocorrelation goes to zero.

From the decay of the autocorrelation curve is possible to obtain the value of the diffusion time of the fluorophore, through a fitting process.

From the auto-correlation curve is also possible to get information on the concentration and diffusion coefficient D of the molecule, provided that the size of the observation volume is already known from previous calibration measurements.

Moreover, considering a the signal intensity proportional to the number of fluorophores in the volume, the amplitude of the previous equation in the limit of $\tau \to 0$ corresponds to the inverse number of molecules in the observation volume[12]:

$$G(0) = \frac{<F^2>}{<F>^2} = \frac{<\delta N^2>}{<N>^2} = \frac{1}{<N>} \tag{2.8}$$

The concentration of fluorophores in FCS experiments has to be kept small because of two main reasons.

First of all, the fluctuation of molecules in and out of the observation volume must be significant; second, the amplitude of the autocorrelation goes as 1/N, which implies that the value of N must be small in order to obtain a significant value.

On the other side, it's also important to remember that the fluctuations must exceed the background noise so we need a trade-off and that's why the suitable concentration is limited to a subnanomolar to a micromular range (from 0.1 to 1000 molecules in the volume) [12].

An analytical expression for a single diffusion time in three dimension can be written as

$$G(\tau) = \frac{1}{N}\left(\frac{1}{1+\frac{\tau}{\tau_{diff}}}\right)\left(\frac{1}{1+\left(\frac{r_0}{z_0}\right)^2\frac{\tau}{\tau_{diff}}}\right)^{\frac{1}{2}} \tag{2.9}$$

under the assumption of a 3D Gaussian detection volume and the absence of blinking.

The characteristic diffusion time, given by

$$\tau_D = \frac{r_0^2}{4D} \tag{2.10}$$

represents the time that the molecule spends in the volume. This value can be estimated for pure single component diffusion by the time τ at which the autocorrelation amplitude has decayed to half its value. The effective detection volume is given by

$$V_{eff} = \pi^{\frac{3}{2}} r_0^2 z_0 \tag{2.11}$$

2.5.2 Experimental set up

A typical FCS set up is shown in figure 2.9 and is based on a confocal microscope.

The beam of excitation is initially parallel and is coupled into a microscope. The beam is then directed onto the back aperture of the objective via a dichroic mirror. There are different types of objectives, such as water or oil immersion, chosen according to the environment of the analyzed sample. The dichroic mirror, together with an emission filter, allow to separate the fluorescence from the spurious excitation light. A properly selected bandpass filter is used to reduce the background, increase the S/N ratio and exclude unwanted optical effects such as Raman signal etc. The fluorescence beam is focused on a confocal pinhole aperture in the image plane in order to reach a diffraction limited detection volume and reject light from outside the focal plane. Finally, the fluorescence signal is focused onto the detector and is correlated. The size of the detection volume depends on the objective used, the wavelength of the laser and the beam diameter at the back aperture of the objective (the smaller the beam, the larger the excitation volume).

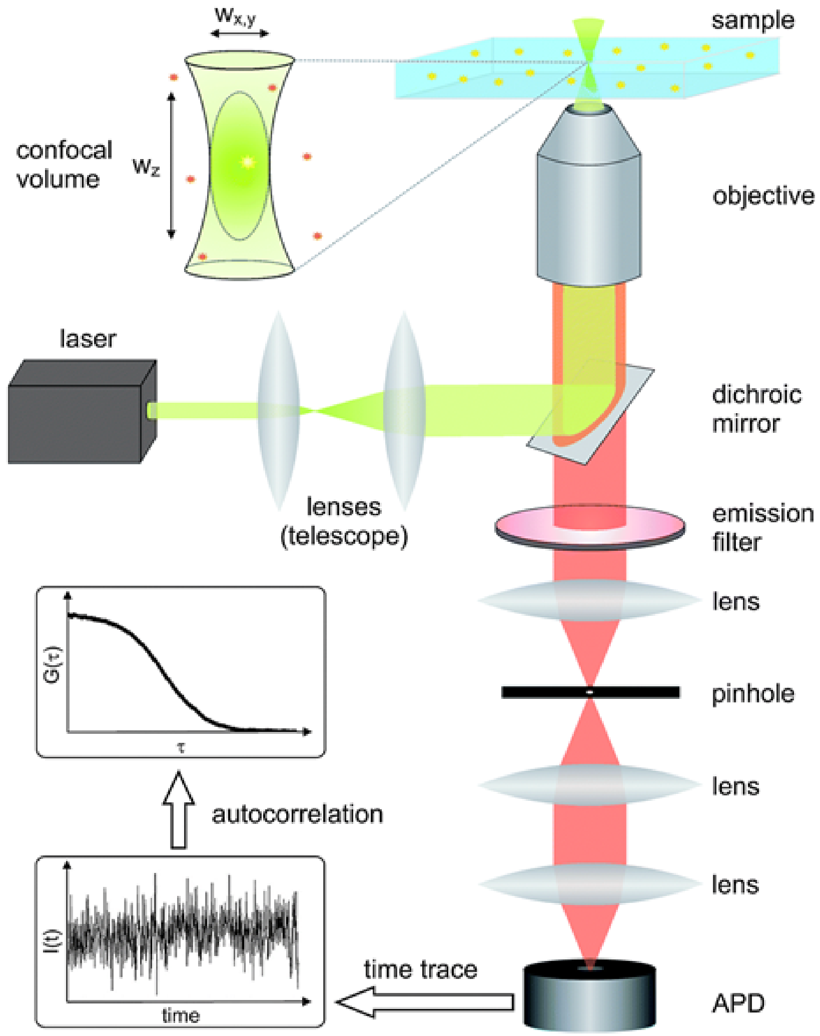

Figure 2.9: Representation of a fluorescence correlation spectroscopy measurement set up.

There can be many sources of artifacts in the measurements, such as pinhole dimension and the cover slide thickness. It is important to optimize the pinhole diameter as it influences the accuracy of the detection of the photon counts per molecule and the S/N ratio. If this value is not optimized, the Gaussian approximation for the detection volume becomes inaccurate, which results in a deviation of the autocorrelation curves from the fit model, reducing the apparent molecular brightness.

With the term cover slide we refer to the thickness of the sample holder (SISTEMA). This parameter needs to be optimized for every cover slide used as discrepancies in the adjustment lead to deviations in the determined diffusion time and concentration due to chromatic and spherical aberrations. The fluorescence intensity signal needs to be recorded by detectors with high quantum efficiency and single-photon sensitivity. Avalanche Photo-Diodes (APD) are usually employed.

The fluorescence intensity data from the detector is correlated either by hardware or software correlators.

2.6 Diffusion of molecular tracers in polymeric matrices

As explained in the introduction, the goal of this thesis work is to study how the movement of small molecular tracer is influenced by the variation of some fundamental parameter of polymeric matrices, such as glass transition temperature and molecular weight.

The diffusion of molecules and molecular tracers in polymeric matrices has been widely studies over the past years as, apart from the fundamental basic interest, this diffusion process is also interesting from a technological point of view. The molecular transport of small molecules influences the mixing of plasticizers with polymers, the removal of residual monomer or solvent from polymers through the devolatilization process, and the formation of films, coatings and foams from a polymer-solvent mixture. [21, 22]

The diffusion of small molecules in polymers matrices is generally analyzed using free volume theories and considering the segmental dynamics of the polymeric matrix. [23]
The basic assumption in the free volume theory is that the molecular transport relies on a continuous redistribution of free volume elements within the liquid and that the availability of free volume within the system controls the molecular transport.
Free volume is an inherent property of the polymer matrix that arises from the free spaces between entangled polymer chains, which can not be directly observed as they are at the molecular scale. These free volume openings are intrinsically dynamic and transient since the size (and existence) of any individual free volume depends on the vibrations and translations of the surrounding polymer chains. The translational motion of the polymer chains can open and close and can form open/close channels, providing “pathways” for diffusion jumps.[23]

Between the main parameters that can influence the motion of small molecules in polymers there are segmental mobility, glass transition temperature and molecular weight. [21, 22, 23]

The segmental mobility of the polymer plays a significant role in the diffusion process and is strongly influenced by the presence of rigid structures in the backbone (such as double or triple bonds), bulky side groups or bulky/rigid chain ends. The stronger the presence of these elements, the more the polymer segmental motion is hindered, creating large and possibly interconnected free volume elements in the polymer matrix.

As said, also the variation of molecular weight influences the diffusion of small tracers in a matrix. This is because the higher the molecular weight, the longer are the chains. From one point of view, longer chains mean that the chain ends represent a lower percentage of the overall systems and this can enhance the ability of a tracer to diffuse through the system, especially when the chain ends are rigid and bulky groups that block the mobility of the polymer. On the other hand, the longer the chains, the more prone to entanglement the system is. Chain entanglement is a kind of physical link that polymeric chains can form and happens when long chains are contained in a more or less small volume and they tangle with each other, hindering the overall flow of the system. The physical definition of entanglement is very simple: if the chain crosses an arbitrary plane 3 times, then it is entangled (depicted in figure 2.10). This is because if one tries to pull a chain in this configuration, it will necessarily trap another polymer chain in a different place.

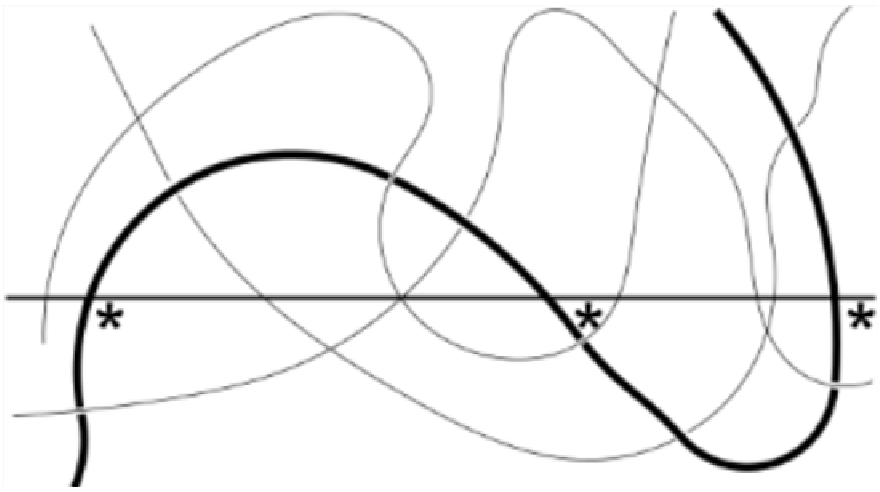

Figure 2.10: Entanglement of a polymeric chain, marked as *, over an arbitrary plane.

The number of chain segment crossings per unit area is independent of molecu-

lar weight, but the number of chains intersecting the plane decreases with increasing molecular weight. Thus, by varying the molecular weight, we can reach a state where the number of bridges is comparable to the number of chains. [23]
This entanglement hinders the motion of small molecular tracers in the polymeric matrix: the higher the molecular weight, the higher the level of entanglement, the less the free volume. All of this means that the molecular tracers don't have much space to move and their diffusion times become longer.

A third important parameter to keep in mind when talking about diffusion in polymers is glass transition temperature (Tg), which is the transition between a highly viscous brittle structure (glassy) and less viscous mobile structure (rubbery). Depending on this value, a material can exhibit a glassy or amorphous character.
The rubbery state represents a liquid-like structure with high segmental motion, resulting in an increase in the free volume with temperature. The mobility of a polymer chain decreases below and increases above the glass transition temperature. The diffusion time of a small molecules is highly influenced by the Tg of a polymer and by the difference between the temperature of the system and the Tg of the polymer. The further away from the Tg value, the less viscous is the system and the easier is for a tracer to move though it.

Of course all of these parameters have to be considered taking also into account the dimension (hydrodynamic radius) of the tracer.

One of the goals in this work is try to get a deeper understanding of how glass transition temperature and molecular weight influence the diffusion of small molecular tracers in polymers using fluorescence spectroscopy measurements.

Chapter 3

Experiments and Materials

In this chapter the chemicals and materials ,as well as the analytical setups that were used for this work, are summarized. Furthermore, the experiments with all the important parameters are described in detail.

3.1 Materials

The molecular rotor LBX37 was dispersed in different polymeric matrices in order to determine its diffusion times and lifetimes. Four different polymers were studied according to their glass transition temperature, availability of a good range of molecular weights and their compatibility with organic solvents.
Uvasol® spectroscopic grade chloroform (>99.0%) was purchased from Sigma Aldrich and was used as a solvent to prepare all the samples.
The molecular rotor LBX37 was provided in a $5{\cdot}10^{-4}$M solution in chloroform from the group of Roberto Simonutti (Department of Materials Science, University of Milano-Bicocca, Italy).

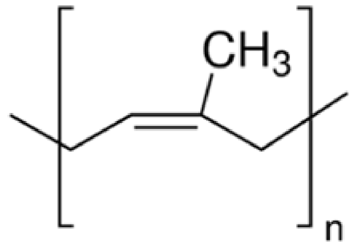

Figure 3.1: Structure of poly(isoprene)

3.1.1 Poly (Isoprene)

Polyisoprene elastomers are currently being used in a variety of applications requiring good resilience, low water swell, high gum tensile strength, good tack and high hot tensile strength. The largest end use for polyisoprene by far is in tires. Black-loaded polyisoprene finds uses in tires, motor mounts, pipe gaskets, shock absorber bushings, and many other molded and mechanical goods. Gum polyisoprene compounds are used in rubber bands, cut thread, baby bottle nipples, and extruded hoses, and other such items. Mineral-filled polyisoprene finds applications in footwear, sponges, and sporting goods. Other important uses include medical applications and adhesives and sealants.

3.1.2 PDMS

Polydimethylsiloxane (PDMS) belongs to a group of polymeric organosilicon compounds that are commonly referred to as silicones. PDMS is the most widely used silicon-based organic polymer, and is particularly known for its unusual rheological (or flow) properties. PDMS is optically clear, and, in general, inert, non-toxic [29], and non-flammable. Its applications range from contact lenses and medical devices to elastomers; it is also present in shampoos (as dimethicone makes hair shiny and slippery), food (antifoaming agent), caulking, lubricants and heat-resistant tiles.

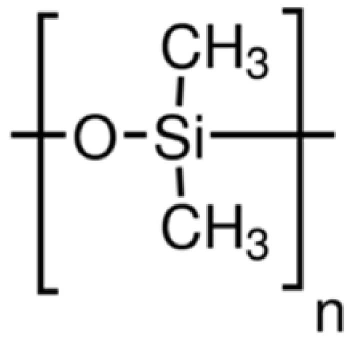

Figure 3.2: Structure of poly(dimethyl siloxane)

The PDMS used in this work was purchased from PSS Polymer Standards Service GmbH (Germany).
The different molecular weight purchased, as well as their PDI, are reported in table 3.1.

3.1.3 Poly (1,2-butadiene)

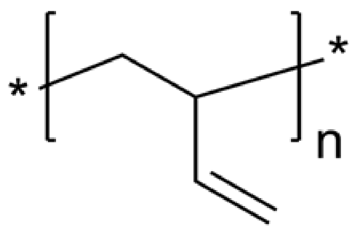

Figure 3.3: Structure of poly(1,2 butadiene)

Polybutadiene rubber is a polymer formed from the polymerization of the monomer 1,3-butadiene. Polybutadiene has a high resistance to wear and is used especially in the manufacture of tires, which consumes about 70% of the production. Another 25% is used as an additive to improve the toughness (impact resistance) of plastics such as polystyrene and acrylonitrile butadiene styrene (ABS).

Table 3.1: This table reports the range of molecular weight used as well as the source, their PDI and the grass transition temperature.

Molecular weight	Source	PDI	Tg
162	PSS	1.12	-120°C
237	PSS	1.12	-120°C
311	PSS	1.12	-120°C
1k	PSS	1.12	-120°C
1.5k	PSS	1.12	-120°C
5k	PSS	1.12	-120°C
16k	PSS	1.12	-120°C
18k	PSS	1.12	-120°C
20k	PSS	1.12	-120°C
32k	PSS	1.12	-120°C
50k	PSS	1.12	-120°C

It is also used to manufacture golf balls, various elastic objects and to coat or encapsulate electronic assemblies, offering high electrical resistivity.

3.1.4 Poly (butyl acrylates)

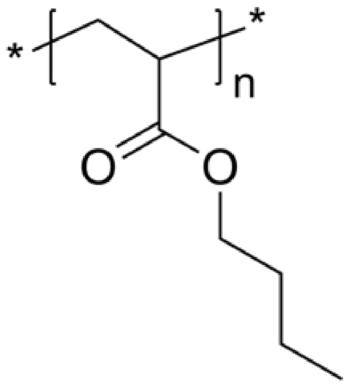

Figure 3.4: Structure of poly(butyl acrylate)

Polyacylates are an important class of polymers that are soft, tough and rubbery. Their glass transition temperature is well below room temperature. They are known for their high transparency, good impact toughness and elasticity, and have fairly good heat resistance up to ca. 450 K under dry heat. They also have good weatherability and ozone resistance since they do not have double bonds in the backbone. Major applications are coatings, paints, textiles, leather finishing, automotive products, tape adhesives, and oil-resistant and high-temperature-resistant elastomers. They are also used as comonomers to increase the plasticity of rigid and brittle plastics.

In this work four different samples of poly(butyl acrylate) were used. The molecular weights are reported in table 3.2. The samples were synthetized using RAFT polymerization at the University of Milano Bicocca by courtesy of Prof. Simonutti's group.

Table 3.2: PBA

Molecular weight	Source	PDI	Tg
5k	UniMiB	1.12	-50°C
7k	UniMiB	1.12	-50°C
11k	UniMiB	1.12	-50°C
18k	UniMiB	1.12	-50°C

3.1.5 Time-Correlated Single Photon Counting

Time-correlated single photon counting (TCSPC) data were recorded on a confocal setup. A PicoQuant diode laser (405 nm) was coupled into a Zeiss LSM 880 microscope (Carl Zeiss, Jena, Germany) through a MBS405 dichroic mirror (Carl Zeiss, Jena, Germany). The laser beam was focused into the sample solutions using a Zeiss C-Apochromat 40×/1.2 W water immersion objective. Emitted fluorescence light was collected by the same objective after passing through a pinhole and a band pass filter EM525/50 (Chroma Technology, Vermont, USA), it is then detected by a PDM SPAD (Micro Photon Devices, Bolzano, Italy) and processed using a TimeHarp 260.

Attofluor® cell chamber (Invitrogen, Paisley, UK) was used as a sample holder for organic solutions and dried samples. The focus of the beam was positioned 20μm above the glass surface and inside the solution. Analysis of the TCSPC data was performed using the PicoQuant SymPhoTime 64 software. The instrument response function (IRF) was reconstructed with the PicoQuant SymPhoTime 64 software by directly evaluating the onset of the decay.

Every measurement, unless different specification, was carried for 180s. The experiment was repeated three times.

3.1.6 TCSPC Measurements of LBX37 in chloroform

A 500 nM solution of LBX37 in toluene was prepared. The sample was measured in an Attofluor® cell chamber at room temperature (T = 22 °C). The setup specifications are described in section 3.1.5. The sample was measured for 120 s and the resulting decay curve was fitted with a single exponential reconvolution fit (see equation 1). The experiment was repeated five times.

3.1.7 TCSPC Measurements of Atto425 in water

A 50 nM solution of Atto425 in water was prepared. The sample was measured in a NUNC chamber at room temperature (T = 22 °C). The setup specifications are described in section 3.1.5. The sample was measured for 120 s and the resulting decay curve was fitted with a single exponential reconvolution fit (see equation 1). The experiment was repeated five times.

3.1.8 Fluorescence Correlation Spectroscopy experiment

FCS experiments were performed on an LSM 880 (Carl Zeiss, Jena, Germany) setup. Excitation laser light was focused on the samples using a Zeiss C-Apochromat 40×/1.2 W water immersion objective. Emission was collected with the same objective and, after passing through a confocal pinhole, directed to a spectral detection unit (Quasar, Carl Zeiss). In this unit, emission is spectrally separated by a grating element on a 32 channel array of GaAsP detectors operating in a single photon counting mode. A HeNe laser (λ = 633 nm) was used for excitation of all the samples and emission in the range from 500 to 553nm was detected. An AttoFluor metal chamber was used as a sample cell. For each sample, 3 measurements were performed. Obtained experimental autocorrelation curves were fitted with a theoretical 2D model function.

Each measurement was made of 20 repetitions, each of which lasted for 20s. The experiment was repeated three times.

3.1.9 FCS measurements of PDI in THF

3.1.10 FCS and TCSPC Measurements of Molecular Rotor in Polymeric Matrices

100mg of every polymer were dissolved in 10μm of chloroform.
The solvent used for PI, PDMS and polybutadiene contained the molecular rotor LBX37 in a concentration of 10^{-8}M.
For PBA samples solvent with two different concentration of rotor were used: 10^{-7}M used for FCS measurements and 10^{-6}M used for TCSPC measurements. The reasons behind this choice are explained in section 4.1.6.
For each polymer, a solution was obtained by stirring for 24h at 600rpm at room

temperature to obtain a good dispersion of the rotor in the polymer. The solution was then placed in an Attofluor chamber whose diameter, of around 2 cm, was reduced using a rubber ring of 0.5 mm of diameter, with a metal weight on top to avoid leaking of the solution. The solution was then placed in an oven at 50°C under high vacuum for 24h in order to make the solvent evaporate.

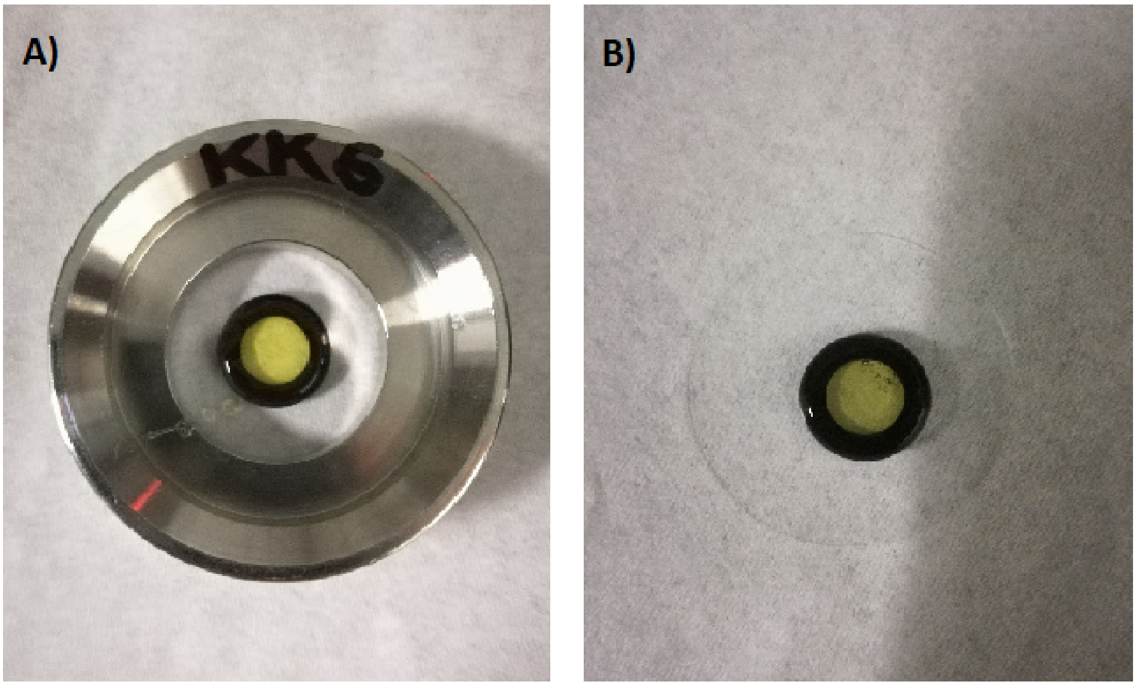

Figure 3.5: PBA sample in Attofluor chamber after 24h in oven

Chapter 4

Result and Discussion

Fluorescence correlation spectroscopy and time-correlated single photon counting measurements were performed on poly(isoprene), poly(dimethyl siloxane), poly(1,2-butadiene) and poly(butyl acrylate).
In this project the idea is to compare how diffusion times and decay times of the LBX37 molecular rotor vary according to molecular weight and glass transition temperature.

4.1 Fluorescence Correlation Spectroscopy and Time-Correlated Single Photon Counting measurementes

4.1.1 TCSPC Measurement of Molecular Rotor in Chloroform

The behaviour of a fluorescent molecular rotor was used to studied in different polymer solution.

This rotor is called LBX37 and is composed of a naphthalene part, acting as the electron-acceptor, and a dibenzoazepine part, which is the electron-donor (figure 2.4). Its fluorescence lifetime depends on the microenvironment, mostly defined by the viscosity (see section 2.2).

To understand the behavior of the rotor, the fluorescence lifetime was first measured in pure chloroform. Chloroform was chosen because it is a good solvent for the molecular rotor and it is suitable for the following experiments on polymeric solutions.

Settings of the experiment are described in detail in section 3.1.5. The fluorescence lifetime was determined using time-correlated single photon counting (TCSPC) experiments. The decay curve of this experiment is pictured in figure 4.1. From the experimental decay a single exponential fit gave a fluorescence lifetime of 0.478ns.

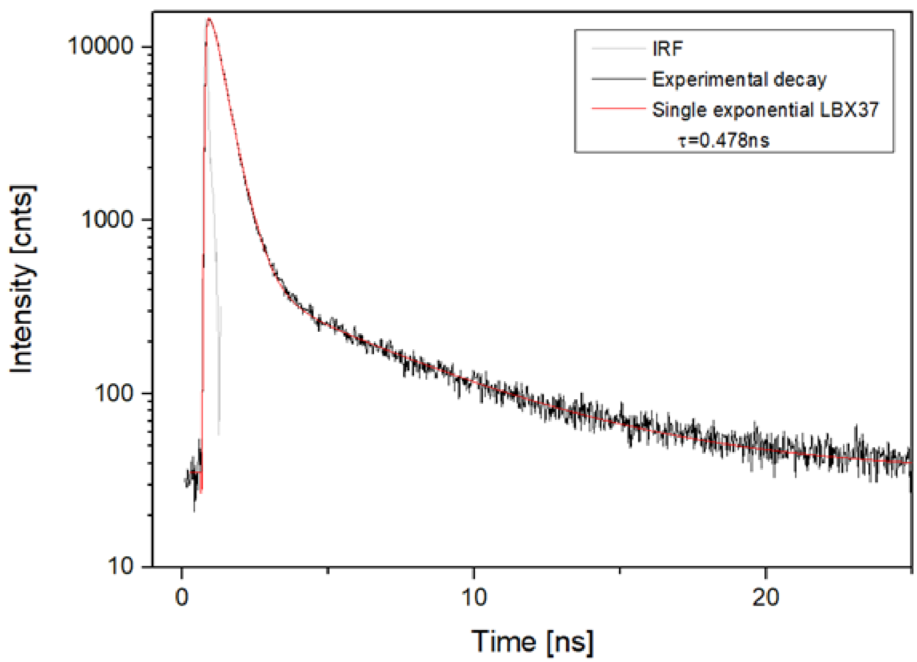

Figure 4.1: Decay shape of LBX37 in pure chloroform. Settings: OD2, 75%, 20μ in, 180s.

The fluorescence lifetime of LBX37 in toluene was quite small compared to conventional fluorescent dyes, such as Atto425. The reason is the special viscosity-dependent behaviour of the molecular rotor (as discussed in section 2.2).
The intramolecular rotation of the molecule is highly efficient in a low-viscosity environment, such as pure chloroform, resulting in a short fluorescence lifetime. To make sur that the method and setup worked correctly, an additional experiment with a fluorescent dye with known fluorescence lifetime was measured. Atto425 is a commercially available fluorescent dye with a reported fluorescence lifetime of τ = 3.6 ns in water.[128] The decay curve of the Atto425 measurement is shown in figure 4.2. The fluorescence lifetime was found to be 3.6 ns, which corresponds to the literture value. This measurement reassured the method for the fluorescence lifetime determination.

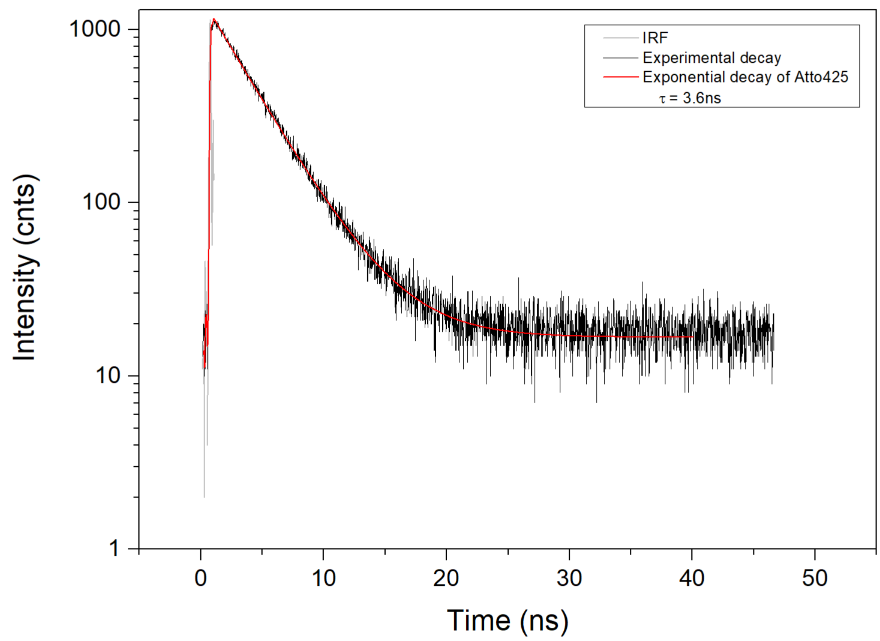

Figure 4.2: Correlation curve of LBX37 in pure chloroform. Settings: OD2, 75%, cv, 20μ in, 20 repetitions of 10 seconds each.

4.1.2 FCS Measurement of Molecular Rotor in Chloroform

To better understand the behavior of the rotor, the diffusion times in polymer solutions were also studied. As a preliminary measurement, the diffusion time of the molecular rotor was measured in pure chloroform.

Settings of the experiment are described in detail in section 3.1.6. The diffusion time was determined using fluorescence correlation spectroscopy (FCS) experiments. The autocorrelation curve of this experiment is pictured in figure 4.3. Experiments were performed on samples with different concentration of molecular rotor in chloroform in order to ..? The reported diffusion time is around 10μs.

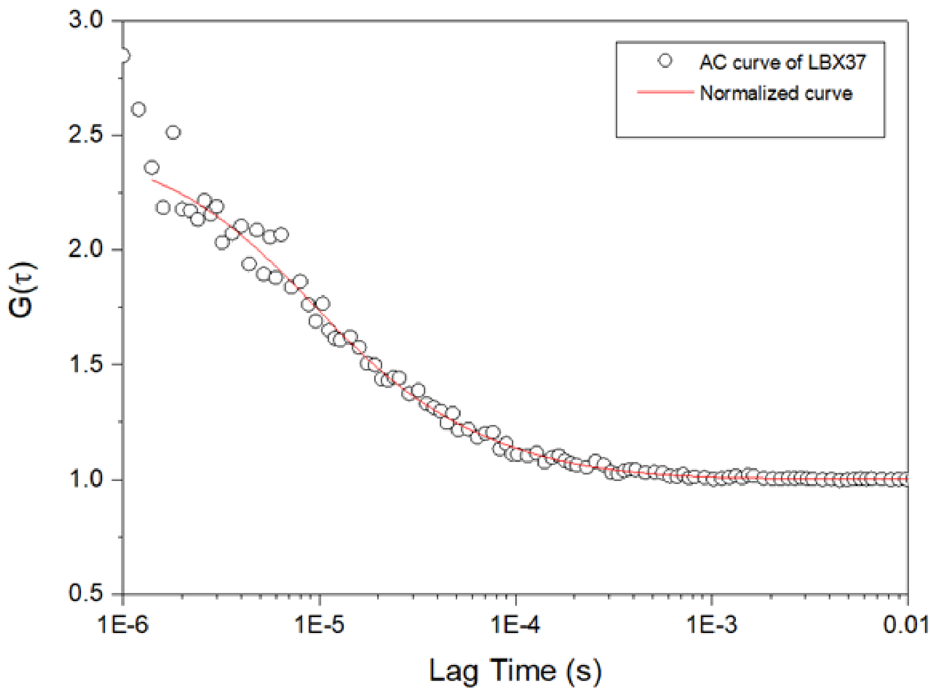

Figure 4.3: Correlation curve of LBX37 in pure chloroform. Settings: OD2, 75%, cv, 20μ in, 20 repetitions of 10 seconds each.

To make sure that the method and setup worked correctly, an additional experiment on Alexa488, a fluorescent dye with known diffusion time,was measured.

Alexa488's reported diffusion time in water is 25μs [metti la reference]. The auto-correlation curve of the Alexa488 measurement is shown in figure 4.4. The diffusion time was found to be ?? ns, which corresponds to the literature value. This measurement reassured the reliability of the diffusion time determination method.

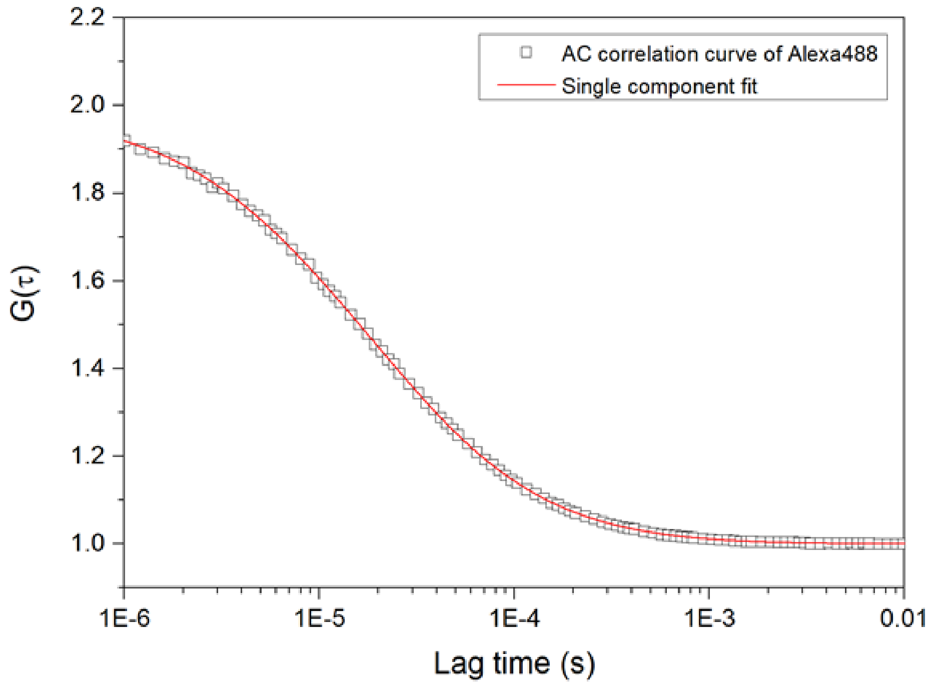

Figure 4.4: Correlation curve of Alexa488 in water. Settings: OD2, 75%, cv, 20μ in, 20 repetitions of 10 seconds each.

4.1.3 Emission spectra of Molecular Rotor

From literature the LBX37 molecular rotor has an emission peak around 500-550nm [7, ESI-rotor].

As the rotor in chloroform was synthetized 4/5 years ago, an emission measurement was performed in order to make sure that no changes in the emission spectrum, due to structural variation or degradation, had happened over time. Two measurements, in pure chloroform, at a concentration of 10^{-6}M, and in poly(butyl acrylate) 11K, with the rotor dispersed at a concentration of 10^{-7}M, were performed.

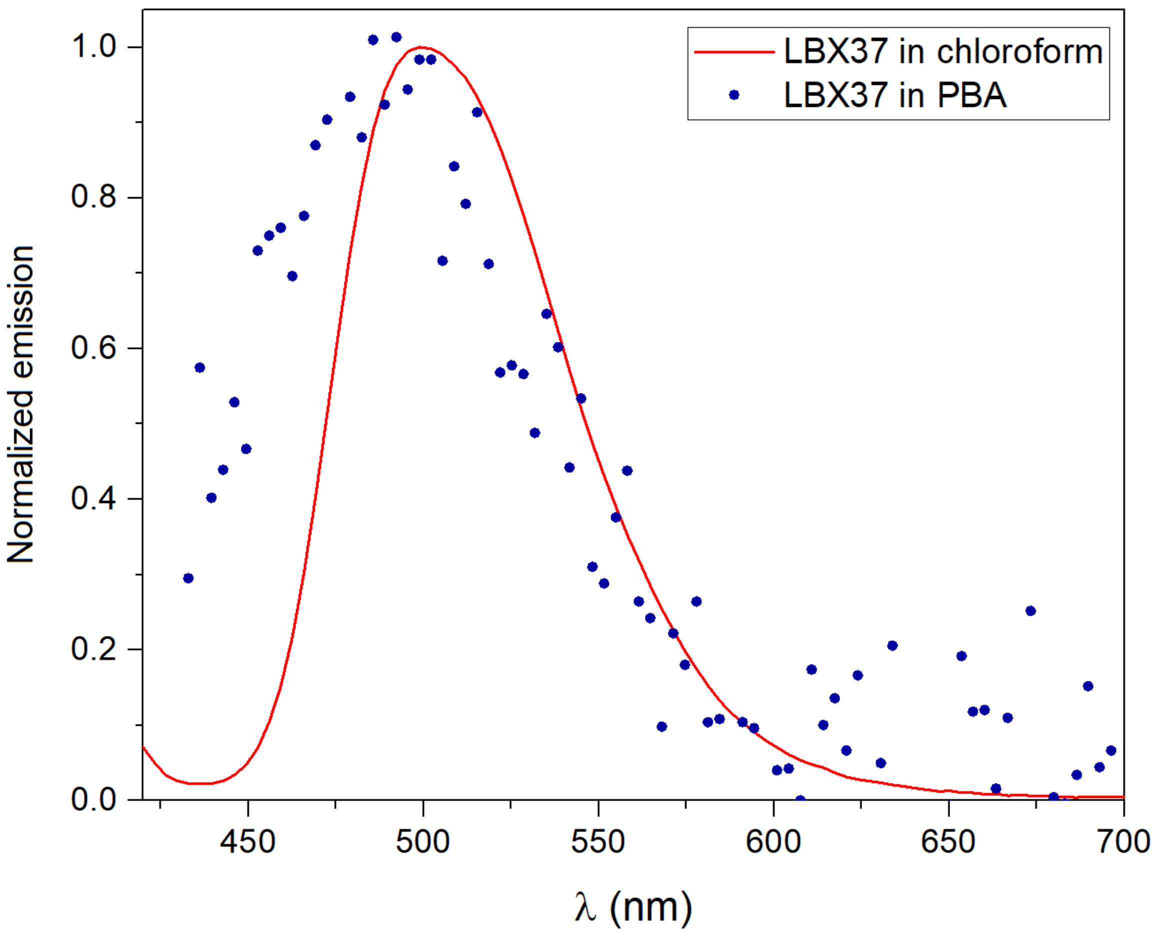

Figure 4.5: Emission spectra of LBX37 in pure chloroform (red line) and in poly(butyl acrylate) with a molar weight of 11k (blue dots).

As shown in figure 4.5, the measurement in pure chloroform reports that the emission range of the rotor is still in the range of 500-550nm, so no degradation accurred during the years.

Also the result from the rotor in polymer experiment showed the same range, even though the data collected is not as precise due to the sample being placed in an o-ring of 0.5mm of diameter, which is not an ideal configuration for the experimental set up.

4.1.4 Poly (Isoprene)

Fluorescence correlation spectroscopy and time-correlated single photon counting were performed on poly(isoprene).

Correlation curves obrained through FCS show no difference between pure poly-

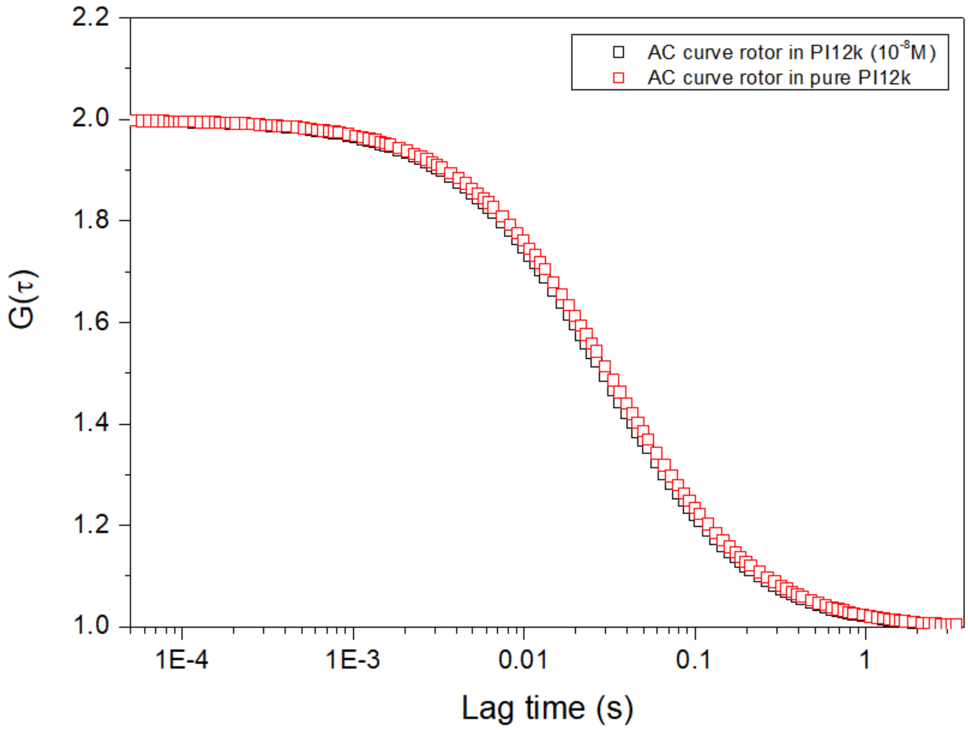

Figure 4.6: FCS PI12k pure and 10^{-8}M

mer and polymer with rotor at a concentration of 10^{-8}M, as shown in figure 4.6. Moreover, also decay time measurements showed that adding rotor doesn't change the diffusion times (figure 4.7.)

These problems are due to the fact that poly(isoprene) shows a strong autofluorescence in the detection range used for measurements, which was also reported in previous studies. [21]

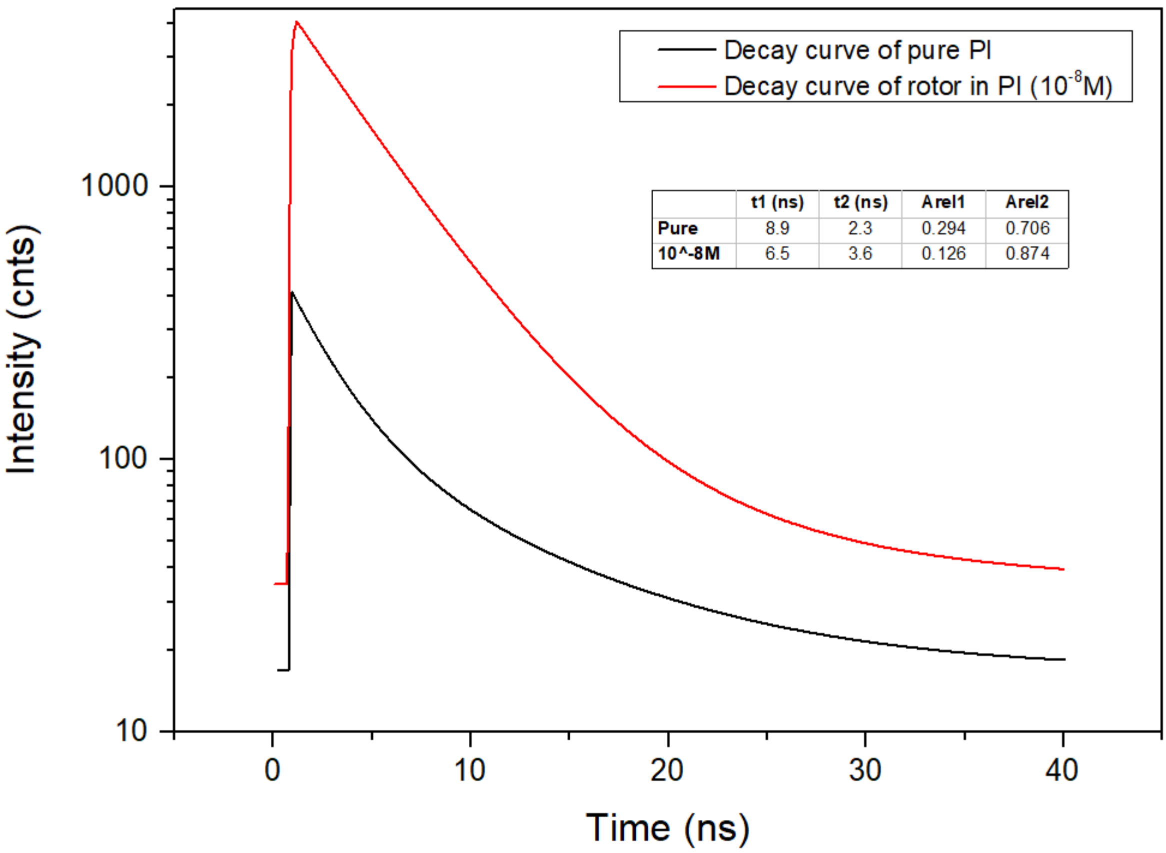

Figure 4.7: FCS PI12k pure and 10^{-8}M

4.1.5 Poly (1,2-Butadiene)

FCS measurements were performed on samples of poly(1,2 butadiene) with different molecular weights.

All the pure polymers showed a correlation, which could be due to the presence of fluorescent species introduced in the system during the synthesis process (stabilizers, impurities..).

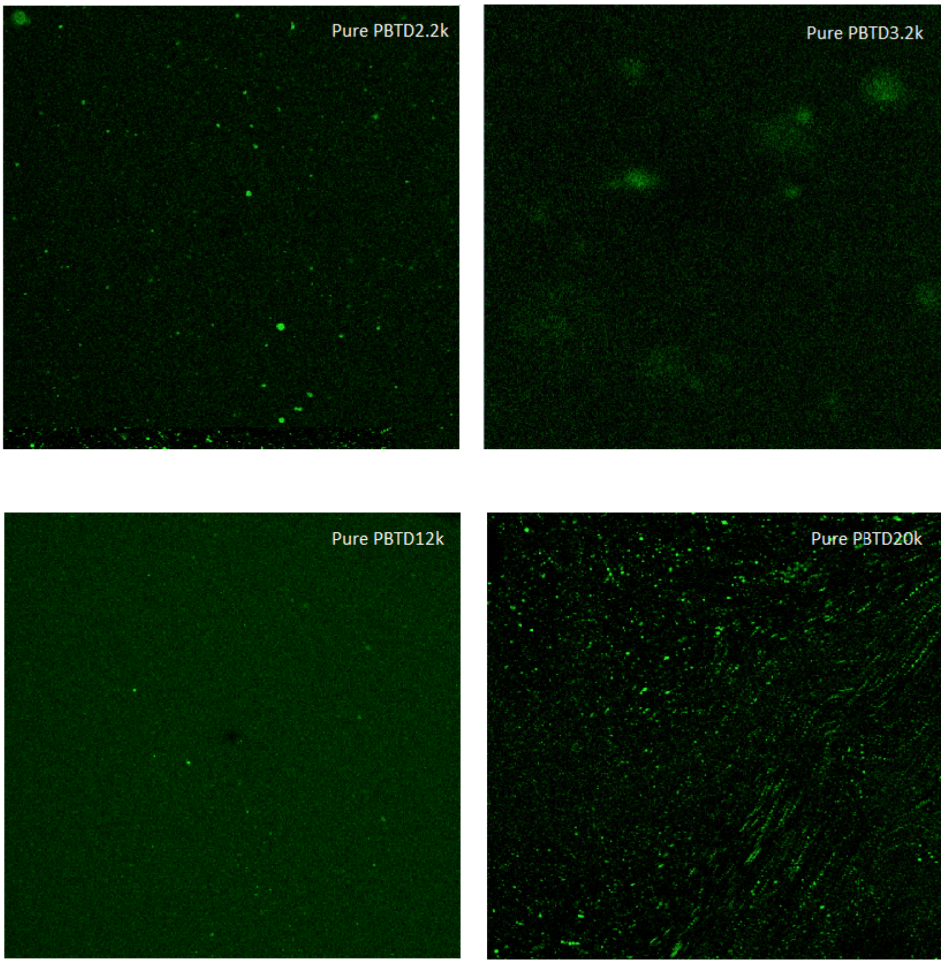

Figure 4.8: Fluorescence imaging of different molecular weights of pure poly(1,2 butadiene) showing fluorescent impurities.

This hypotesis was confirmed by fluorescent imaging of the samples (figure 4.8) which showed the presence of bright spots dispersed in the samples.

Nevertheless, as the count rate of every sample was around 15kHz, it was decided to try to prepare a sample with the rotor to see if it was possible to overcome the contribution due to the pure polymer.

A sample using the polymer with a molecular weight of 1.8K was prepared (procedure described in section 3.1.11), adding the molecular rotor at a concentration of 10^{-8}M. Fluorescent imaging of pure polymer vs sample with the rotor are showed in figure 4.9. Here it is possible to see that some sort of aggregation process happened during the sample preparatio. This makes for unreliable FCS measurements as it is not sure from which component is actually correlated.

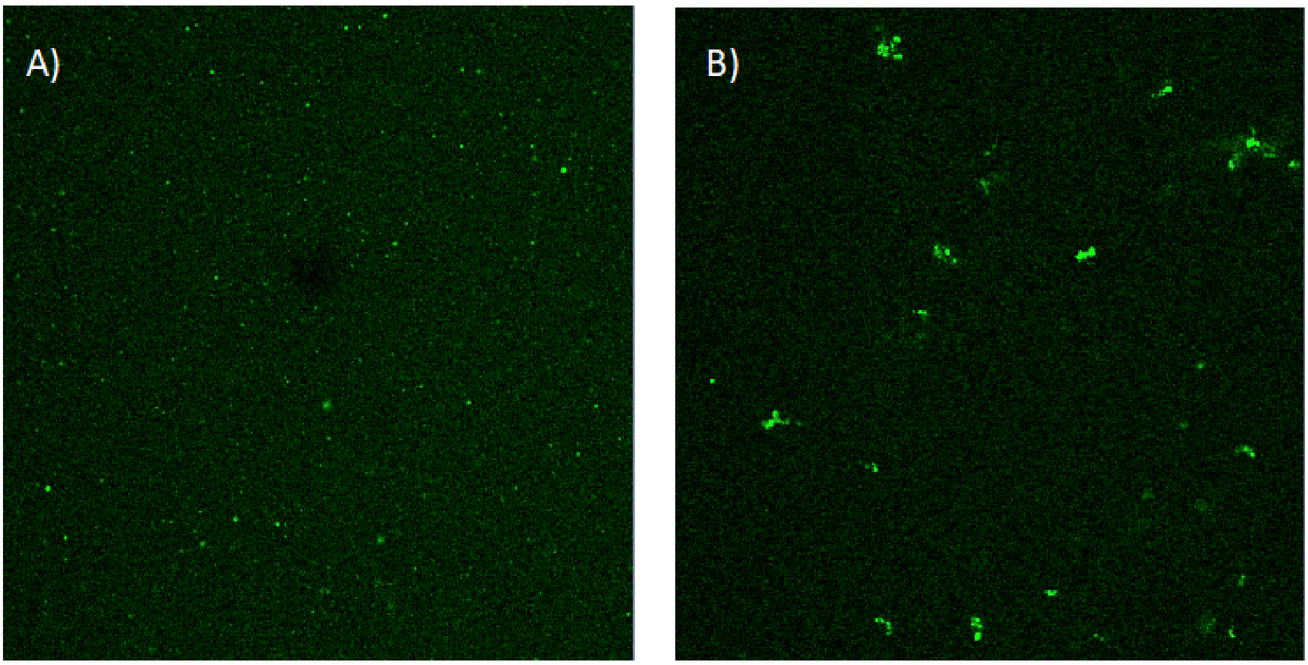

Figure 4.9: Fluorescence imaging of A) pure poly(1,2 butadiene) 12k and B) molecular rotor dispersed in poly(1,2 butadiene) 12k at a concentration of 10^{-8}M.

Samples of poly(1,2 butadiene) with molecular weight of 2.2k and 3.2k with a rotor concentration of 10^{-8}M were also prepared. Unfortunately, during the FCS measurements the polymers showed an increase in the count rate from around 30kHz to over 300kHz in just a few seconds (over measurements of over 400s), which forced the measurement to be stopped before the end. This resulted in unreliable measurements that could not be properly analyzed.

Following the results obtained by these different approaches, it was decided not to continue with further studies on this polymer.

4.1.6 Poly (Dimethyl Siloxane)

The third investigated polymer was poly(dimethyl siloxane), which was possible to obtain on a wide range of molecular weights, as reported in section 3.1.2. Both TC-SPC and FCS measurements were performed on every sample, which was mixed with the molecular rotor at a concentration of 10^{-8}M (preparation process described in section 3.1.11).

From TCSPC measurements decay times were obtained. Results showed a rather constant trend (figure 4.10) meaning that the decay times of the molecular do not follow the bulk polymer viscosity, which increases with Mw.

FCS measurements reported good correlation curves (PDMS non emette in questa zona.. ma dove l'ho letto? Articolo 22?). The diffusion times of the molecular rotor increase with the molecular weight, following the increase of the viscosity.

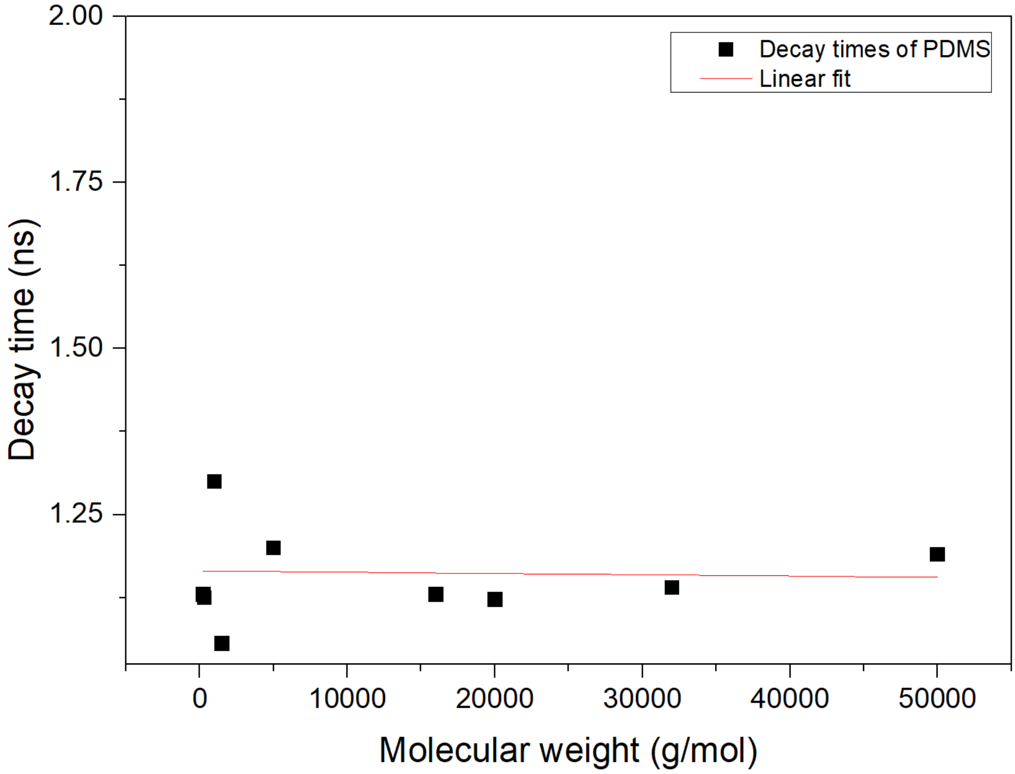

Figure 4.10: Decay times of PDMS samples with a rotor concentration of 10^{-8}M

4.1.7 Poly (Butyl Acrylate)

TCSPC measurements performed on pure polymer reported two decay times, with a predominant very fast component at around τ=0.8ns for each sample, with a reported count rate of around 1kHz. Measurements performed on samples with a rotor concentration of 10^{-8}M reported similar values.
The comparison is reported in figure 4.12.

As a possible solution, a samples with a higher concentration of rotor (10^{-6}M) was prepared. As expected, the count rate was significantly higher for each sample (between 15kHz and 20kHz). The decay times were calculated again using a two-component fitting but the dominant time changed to around 1.6ns. The specific

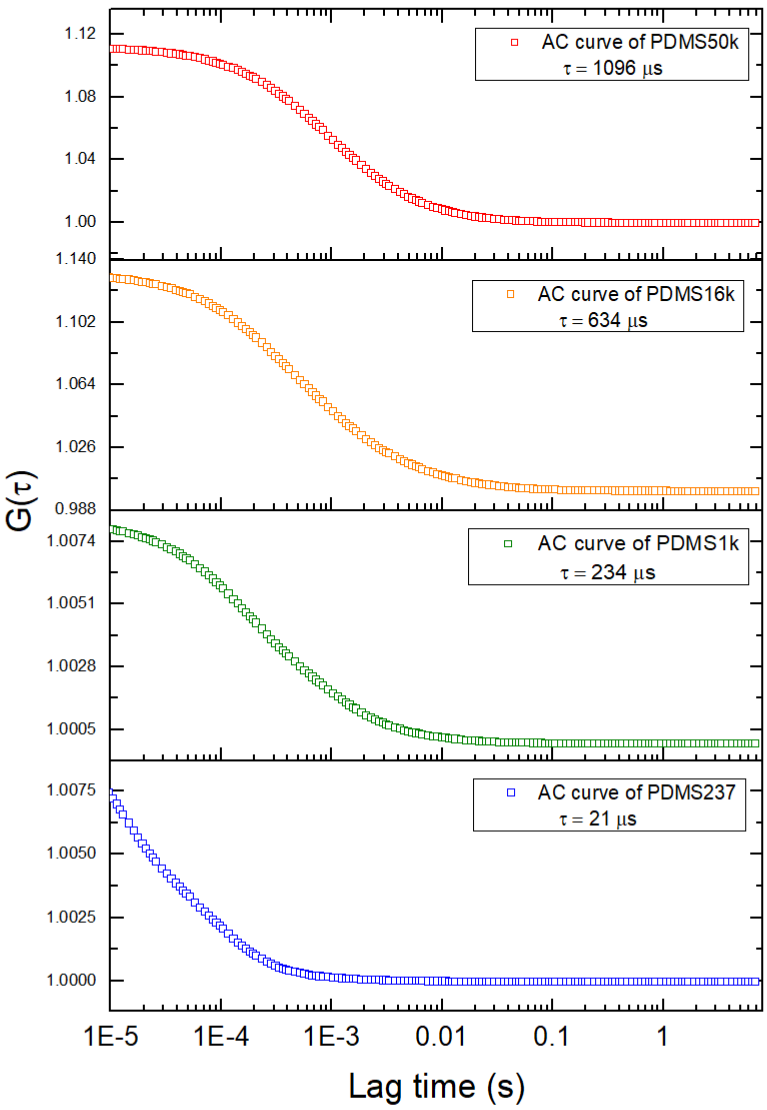

Figure 4.11: Decay times of PDMS samples with a rotor concentration of 10^{-8}M

values obtained for each molecular weight are reported in table 4.1.
Figure 4.13 shows the comparison between the three samples analyzed.

FCS measurements on pure polymer showed a correlation curve but with a count rate of around 20kHz, so the goal was to prepare a sample where the count

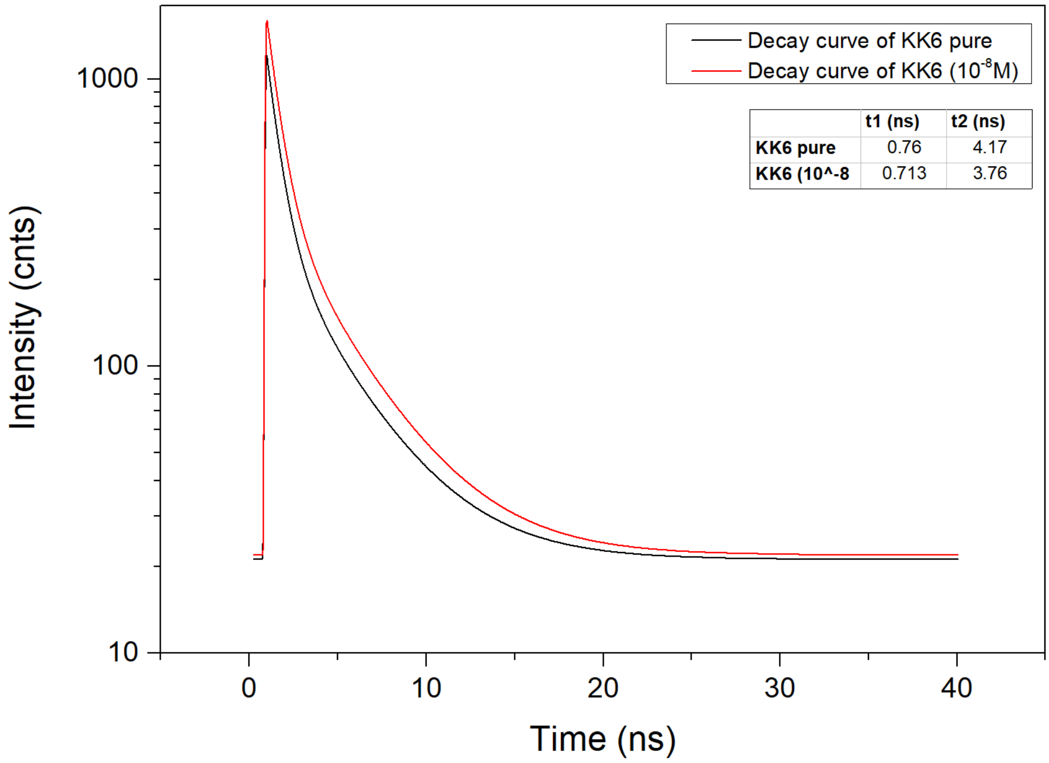

Figure 4.12: Comparision of decay curves obtained for sample KK6 pure (black line), with a concentration of rotor of 10^{-6}M (blue line) and of 10^{-8}M (red line). Settings: OD2, 75%, 20μm in

Table 4.1: Decay times of PBA samples with a rotor concentration on 10^{-6}M

Molecular weight	Decay time (ns)	Tg
5k	1.53	-50°C
7k	1.59	-50°C
11k	1.74	-50°C
18k	1.84	-50°C

rate was high enough so that the contribution from the polymer could be considered non-influent. The measurement obtained from samples with a concentration of rotor of 10^{-8} showed a count rate of around 40kHz which was still not enough

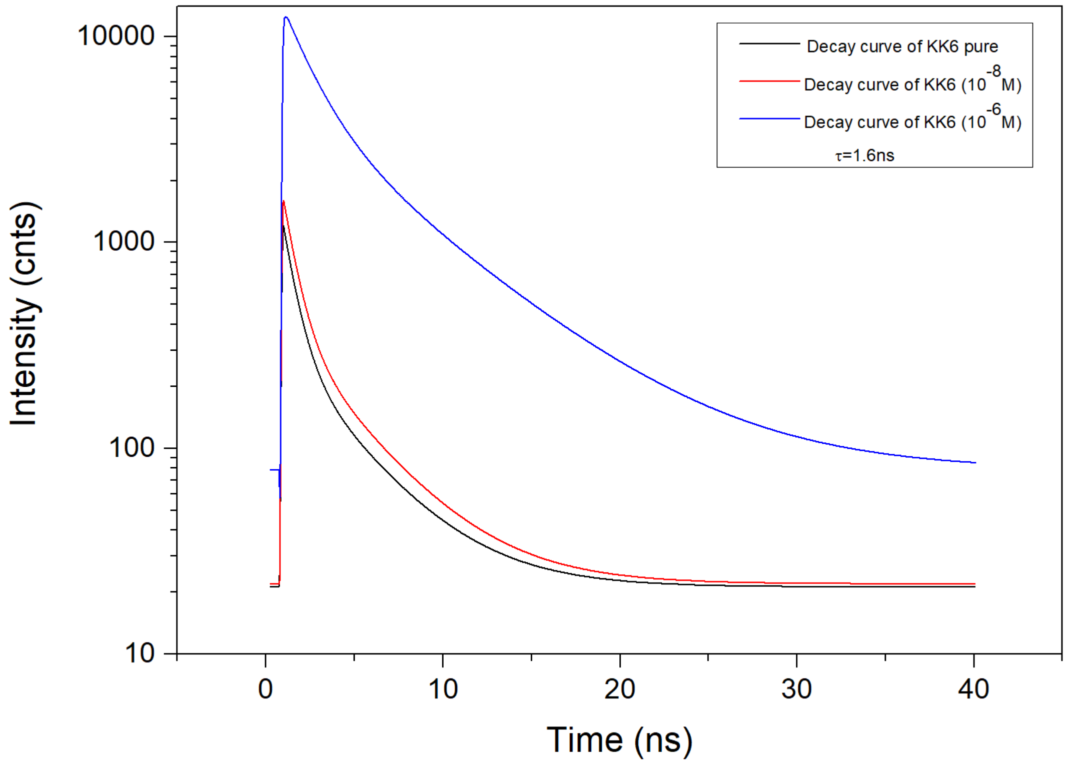

Figure 4.13: Comparision of decay curves obtained for sample KK6 pure (black line), with a concentration of rotor of 10^{-6}M (blue line) and of 10^{-8}M (red line). Settings: OD2, 75%, 20μm in

to determine whether the diffusion times were coming from the polymer or the rotor. The concentration of rotor was then increased to 10^{-7}, showing a count rate of almost 300kHz, allowing to consider the diffusion time as coming from the movement of the rotor.

Comparison FCS curves, as well ad count rate values, are repoter in figure 4.14.

FCS measurements were then performed on all PBA samples prepared with a rotor concentration of 10^{-7}M. The diffusion times, reported in table 4.2, show an increase of the time with the increase of the molecular weight as expected (SISTEMA?)

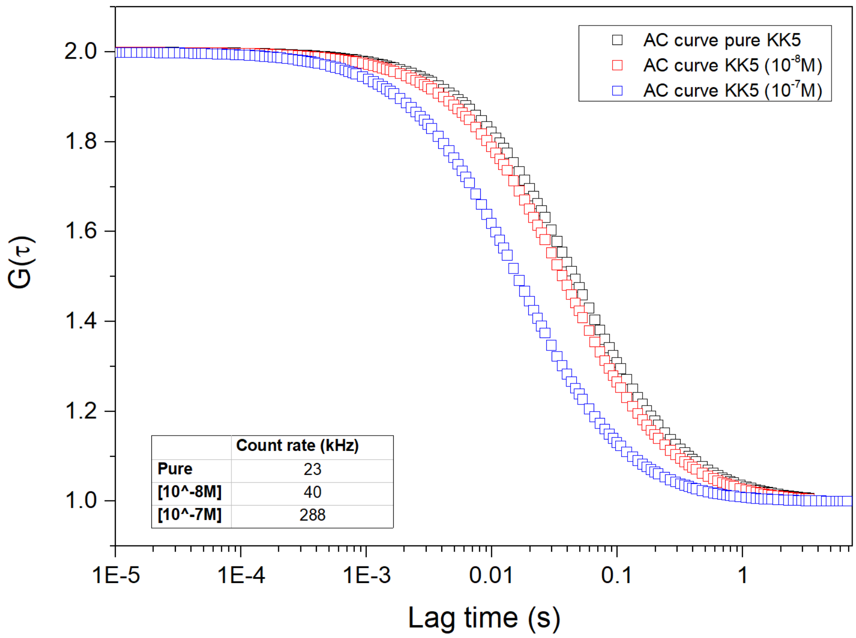

Figure 4.14: Comparision of correlation curves obtained for sample KK5 pure, with a concentration of rotor of 10^{-7}M and of 10^{-8}M. Settings: OD2, 75%, cv, 20μm in.

Table 4.2: Diffusion times of PBA samples with a rotor concentration of 10^{-7}M

Molecular weight	Diffusion time (μs)	Tg
5k	15764	-50°C
7k	20937	-50°C
11k	25133	-50°C
18k	49711	-50°C

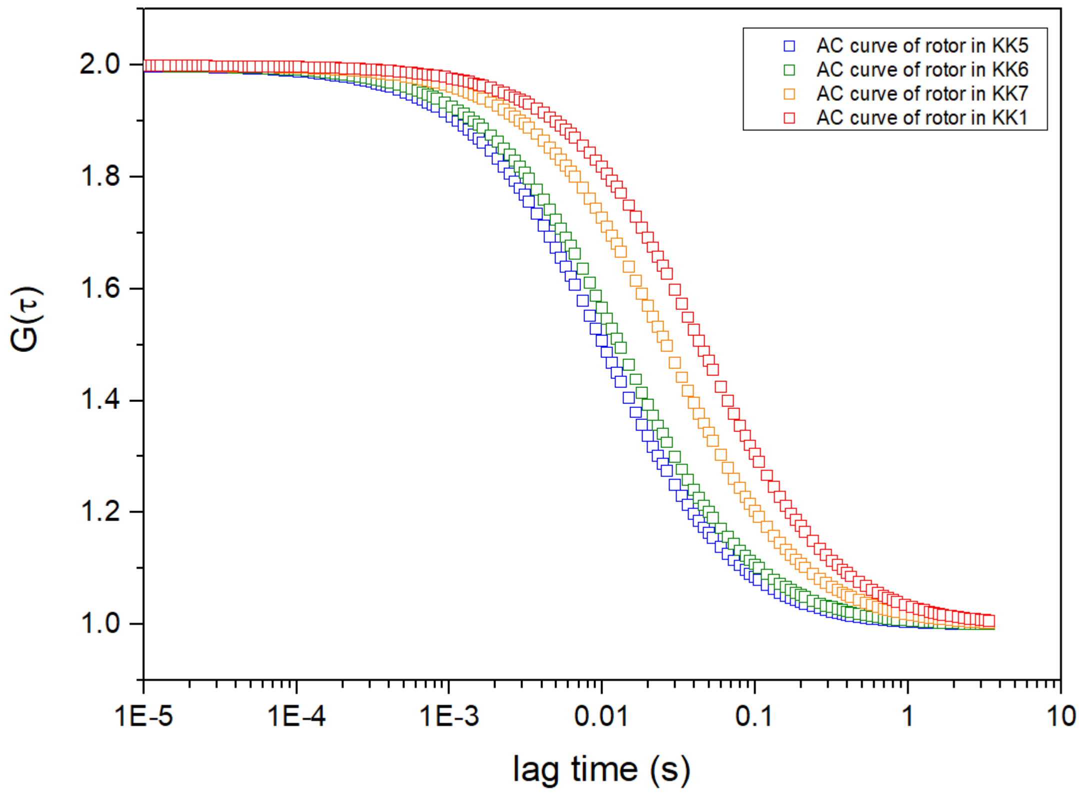

Figure 4.15: Correlation curve of PBA samples

Chapter 5

Conclusions

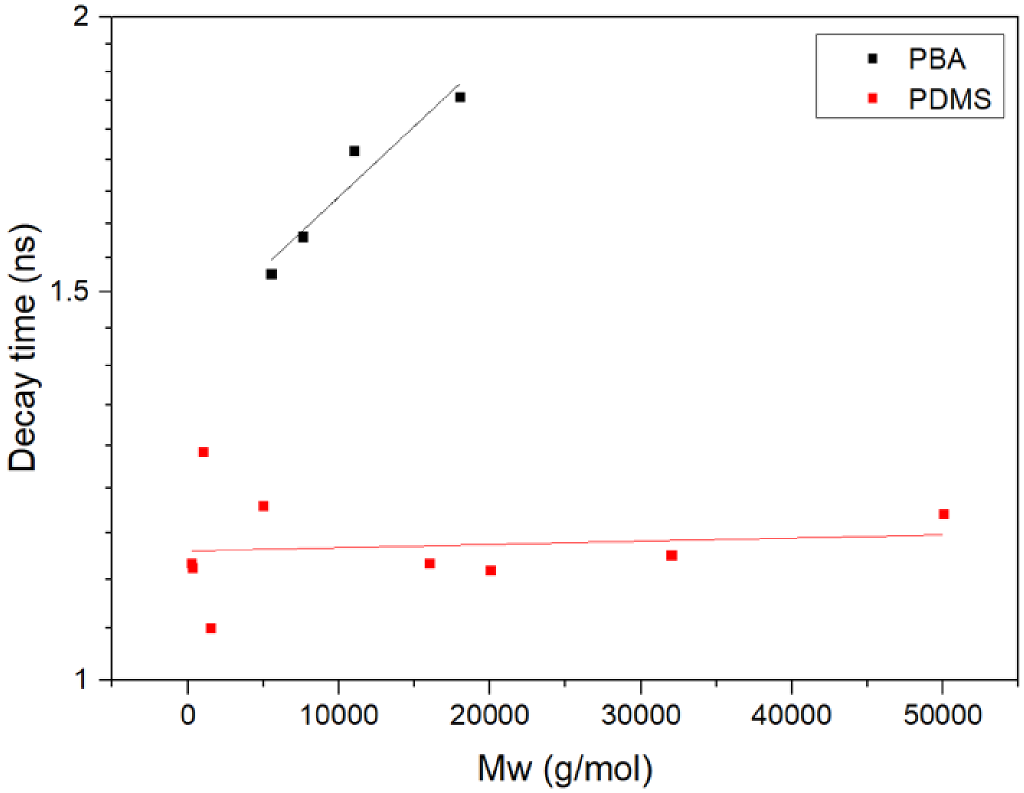

Figure 5.1: Correlation curve of PBA samples

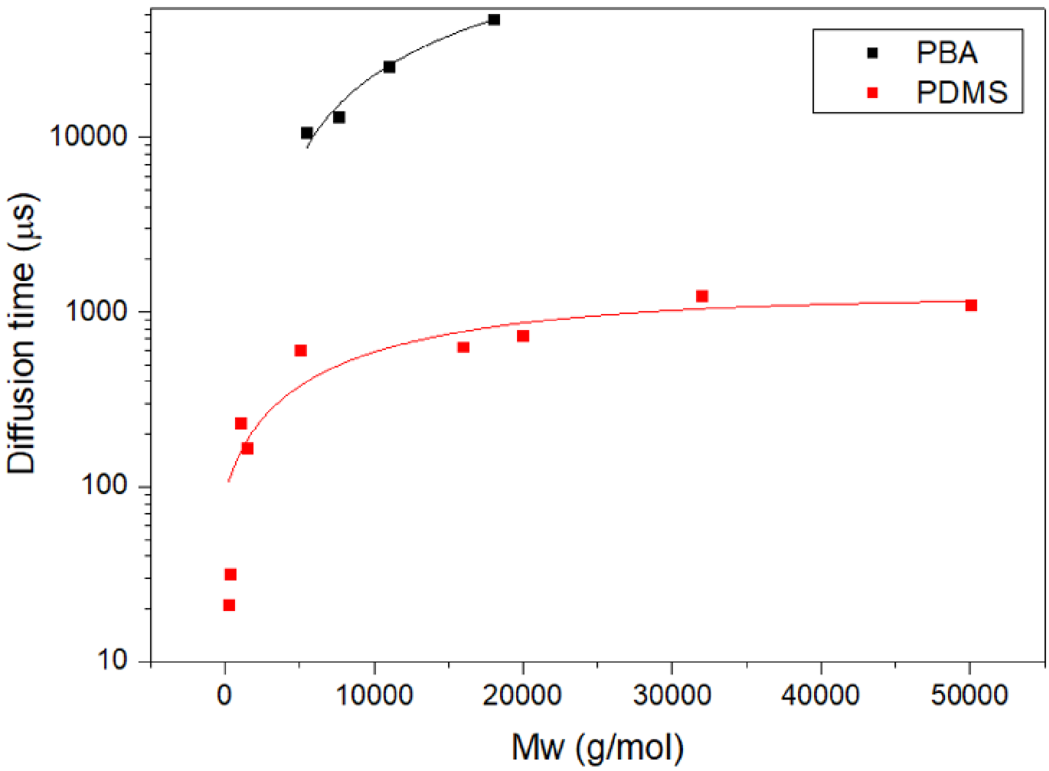

Figure 5.2: Correlation curve of PBA samples

Bibliography

[1] J. W. Lichtman1, J.-A. Conchello, *Fluorescence Spectroscopy*, Nature methods, vol.2, December 2015, p.910-919.

[2] J. R. Lakowicz, "Principles of Fluorescence Spectroscopy",Springer, 2006, p.

[3] Edited by David L. Andrews, *"Encyclopedia of Applied Spectroscopy"*, WILEY-VCH 2009, p.

[4] J. R. Lakowicz, "Principles of fluorescence spectroscopy", ??

[5] W. E. Moerner, D. P. Fromm, *"Methods of single-molecule fluorescence spectroscopy and microscopy"*, Review of Scientific Instruments 74, 2003, p.3597-3619

[6] M. A. Haidekker, E. A. Theodorakis, *"Environment-sensitive behavior of fluorescent molecular rotors"*, Journal of Biological Engineering 2010, p.4-11

[7] G. Vaccaro, A. Bianchi, M. Mauri, S. Bonetti, F. Meinardi, A. Sanguineti, R. Simonutti and L. Beverina *"Direct monitoring of self-assembly of copolymeric micelles by a luminescent molecular rotor"*, Chem. Commun., 2013, 49, p.8474-8476

[8] J. Schultze, *"Polymer-Based Systems for Drug Delivery Studies"*, PhD dissertation, 2017.

[9] S.-C. Lee, J. Heo, H. C. Woo, J.-A. Lee, Y. H. Seo, C.-L. Lee, S. Kim and O-P. Kwon, *"Fluorescent Molecular Rotors for Viscosity Sensors"*, Chem. Eur. J. 2018, 24, 13706 – 13718

[10] T. Cherdhirankorn, *"Diffusion in polymer systems studied by Fluorescence Correlation Spectroscopy"*, PhD dissertation, 2009

[11] S. Sasaki, G. P. C. Drummen and G. Konishi, *"Recent advances in twisted intramolecular charge transfer (TICT) fluorescence and related phenomena in materials chemistry"*, J. Mater. Chem. C., 2012, 4, p.2731-2743

[12] 12. J. Mutze, T. Ohrt and P. Schwille, *"Fluorescence correlation spectroscopy in vivo"*, Laser Photonics Rev. 5, No. 1, 2011, p.52–67

[13] 13. K. Koynov, H.-J. Butt, *"Fluorescence correlation spectroscopy in vivo"*, Laser Photonics Rev. 5, No. 1, 2011, p.52–67

[14] P. Schwille, *"Fluorescence Correlation Spectroscopy - An Introduction to its Concepts and Applications"*, Research Gate, 2014

[15] P. Schwille, J. Bieschke, F. Oehlenschltiger, *"Kinetic Investigations by Fluorescence Correlation Spectroscopy: The Analytical and Diagnostic Potential of Diffusion Studies"*, Biophysical Chemistry 66, (1997), p.211-228

[16] M. Wahl, *"Technical notes: Time-Correlated Single Photon Counting"*, PicoQuant GmbH, berlin

[17] W. Becker, A. Bergmann, G. Biscotti, A. Rück *"Advanced time-correlated single photon counting technique for spectroscopy and imaging in biomedical systems"*

[18] D. B. Murphy, *"Fundamentals of light microscopy and electronic imaging"*

[19] S. W. Paddock, *“Confocal Laser Scanning Microscopy”*, BioTechniques 27, 1999, p.992-1004

[20] M. Minsky, *“Memoir on Inventing the Confocal Scanning Microscope”*, Sanning Vol. 10, 1988, p.128- 138

[21] T. Cherdhirankorn, V. Harmandaris, A. Juhari, P. Voudouris, G. Fytas, K. Kremer and K. Koynov, *“Fluorescence correlation spectroscopy study of molecular probe diffusion in polymer melts”*, Macromolecules, 2009, 42, p.4858-4866

[22] A. Vagias, J. Schultze, M. Doroshenko, K. Koynov, H.-J. Butt, M. Gauthier, G. Fytas and D. Vlassopoulos, *Molecular tracer diffusion in nondilute polymer solutions; universal master curve and glass transition effect*, Macromolecules

[23] T. Sabu, W. Runcy, A. Kumar, S. S. George, *"Transport Properties of Polymeric Membranes"*, Elsevier, 2017, p.6-9

[24] G. Wypych, *"PVC degradation and stabilization"*, ChemTec Publishing, 2015, p.47-75

[25] P. C. Hiemenz, *"Polymer chemistry"*, CRC press, 2008, p.327-381

[26] T. Cherdhirankorn, G. Floudas, H.-J. Butt and K. Koynov, *“Effects of Chain Topology on the Tracer Diffusion in Star Polyisoprenes”*, Macromolecules, 2009, 42, p. 9183–9189

[27] D. Ehlich and H. Sillescu, *“Tracer Diffusion at the Glass Transition”*, Macromolecules 1990, 23, p.1600-1610

[28] Marcus T. Cicerone, F. R. Blackburn and M. D. Ediger, *“Anomalous Diffusion of Probe Molecules in Polystyrene: Evidence for Spatially Heterogeneous Segmental Dynamics”*, Macromolecules 1995, 28, p.8224—8232

[29] A. Best, T. Pakula and G. Fytas, *"Segmental Dynamics of Bulk Polymers Studied by Fluorescence Correlation Spectroscopy"*, Macromolecules, 2009, 38, p.4539-4541

[30] S. Maji, O. Urakawa, K. Adachi, *"Relationship between segmental dynamics and tracer diffusion of low mass compounds in polyacrylates"*, Polymer 48, 2007, p. 1343-1351

[31]

[32]

[33] A. Mata, A. J. Fleischman and S. Roy, *"Characterization of Polydimethylsiloxane (PDMS) Properties for Biomedical Micro/Nanosystems"*, Biomedical Microdevices 7:4, 2005, p.281–293

[34]

[35] E. Penzel, N. Ballard and J. M. Asua, *"Polyacrylates"*, Ullman's encyclopedia of industrial chemistry, 2018